Mike Jefferies

Senior Geotechnical Consultant
Golder Associates Ltd.
Canada

Mike Jefferies graduated in civil engineering from King's College (London) and subsequently gained an M.Sc. in soil mechanics from Imperial College (London). He qualified as a charted civil engineer in the UK in 1978; the same year he immigrated to Canada. A registered professional engineer in Alberta and British Columbia, since 1978 Mike has worked for Canadian companies in numerous parts of the world including: Chile, Kyrgyzstan, Lebanon, Jordan, Netherlands, Peru, Portugal, Russia, UK, and USA. Presently a Senior Consultant with Golder Associates, it is Mike's earlier role as supervising engineer with Gulf Canada Resources, then exploring for oil in the Canadian Arctic Offshore, that produced the advances in theoretical soil mechanics underlying this Šuklje Lecture.

While working as a consulting engineer, Mike has contributed to technical progress within civil engineering, authoring or co-authoring some 80 scientific papers that cover: constitutive modelling of soils, insitu soil testing, ground improvement, liquefaction, and ice-induced vibrations of offshore structures. A keynote speaker at international conferences on arctic engineering, hydraulic fill construction, and soil liquefaction, Mike is most known for the 'state parameter' approach to characterizing soils.

Based on his work with Gulf Canada, Mike was recognized with an award for an outstanding and original contribution to ice mechanics. In 2012, following the 2006 publication of his now widely-cited book on soil liquefaction, Mike was the Canadian Geotechnical Society's Cross-Canada Lecturer.

Mike Jefferies je diplomiral na Fakulteti za gradbeništvo na King's Collegeu (London, UK) in zatem naredil magisterij iz mehanike tal na Imperial Collegeu (London, UK). Imenovanje v licenciranega gradbenega inženirja je pridobil v Veliki Britaniji leta 1978 in v istem letu emigriral v Kanado. Kot registrirani profesionalni inženir v Alberti in Britanski Kolumbiji je po letu 1978 delal za kanadske družbe v Čilu, Kirgizistanu, Libanonu, Jordaniji, na Nizozemskem, v Peruju, na Portugalskem, v Rusiji, Veliki Britaniji in ZDA. Trenutno je na položaju starejšega konzultanta v Golder Associates s sedežem v Vancouvru. V preteklosti je delal kot nadzorni inženir za Gulf Canada Resources, ki je črpalo nafto v vodah kanadskega Arktike; omenjeno delo je pripomoglo k napredku teorije mehanike tal, ki bo predstavljena na predavanju na Šukljetovem dnevu.

S svojim delom je Mike Jefferies doprinesel k tehničnemu napredku v gradbeništvu in geotehniki, in sicer kot avtor ali soavtor več kot 80 znanstvenih člankov, ki zajemajo: konstitutivno modeliranje tal, in situ raziskave, izboljšanje tal, likvifakcijo in vibracije obalnih konstrukcij, ki jih je povzročilo delovanje ledu. Kot ključni predavatelj je vabljen na mednarodne konference o arktičnem inženirstvu, likvifakciji tal ter izgradnji nasipov z metodo pluviacije. V strokovni javnosti je Mike Jefferies najbolj znan po svojem prispevku h karakterizaciji obnašanja tal z uporabo ˝parametra stanja˝.

Za svoje delo pri Gulf Canada je Mike prejel nagrado za izjemen prispevek pri raziskovanju mehanike ledu. Na podlagi njegove leta 2006 objavljene izjemne knjige o likvifakciji tal ga je Kanadsko Geotehniško društvo leta 2012 imenovalo za predavatelja na seriji geotehniških seminarjev Cross-Canada Lecture Tour.

Mike JEFFERIES

Senior Geotechnical Consultant
Golder Associates Ltd.
Canada
e-naslov: mike_jefferies@golder.com

SOIL LIQUEFACTION - A MECHANICS VIEW

ABSTRACT: Soil liquefaction has been a concern to civil engineers for more than 100 years, with liquefaction failures in the 19th and early 20th century leading to the first 'liquefaction resistant' dam being constructed 80 years ago. Understanding of the physics and mechanics of liquefaction now reached the point that liquefaction – in all its forms - has become a readily computable behaviour with models based on the state parameter. An interesting aspect is that, while the state parameter approach to characterizing soils developed from observations during hydraulic fill construction in the Canadian offshore, it was based on a line of thinking that starts in 1885 and with contributions from Manchester, Harvard, MIT, Imperial, and Cambridge. The talk will briefly review this history of ideas and work through to the implementation of the state parameter in a constitutive model (equations will be mostly left to the written version…). This model then provides the basis for understanding liquefaction, with examples of static liquefaction being presented. Finally, the talk will discuss how to measure the state parameter in real soil strata, with their intrinsic natural variability, using the CPT. For those interested in trying out the methodology to simulate liquefaction, an Excel spreadsheet will be made downloadable and will be briefly discussed in the talk.

POVZETEK: Likvifakcija tal je problem, s katerim se gradbeni inženirji ukvarjajo več kot 100 let, in sicer zaradi katastrofalnih porušitev izzvanih z likvifakcijo v teku 19. in 20. Stoletja. To je pripeljalo do gradnje prvega jezu pred osemdesetimi leti, ki je bil ˝odporen na likvifakcijo˝. Razumevanje fizike in mehanike likvifakcije v vseh njenih pojavnih oblikah je postalo obnašanje, ki ga lahko izračunamo z modeli, ki so zastavljeni s pomočjo parametra stanja. Zanimiv aspekt je v tem, da čeprav je pristop z uporabo parametra stanja razvit z opazovanjem kompakcije hidravličnih nasipov na kanadskih priobalnih konstrukcijah, je bil njegov razvoj zasnovan na razmišljanju, ki se je začelo leta 1885 in s prispevki, ki so prišli iz Manchestra, Harvarda, MIT-a, Imperiala in Cambridga. V predavanju bo povzeta kratka zgodovina idej in dela na tem področju skozi implementacijo parametra stanja v konstitutivnem modelu. Tovrstni model predstavlja osnovo za razumevanje mehanike likvifakcije. Predstavljeni bodo primeri statične likvifakcije ter prikazane metode za določanje parametra stanja v naravnih tleh, z vso njihovo spremenljivostjo, z uporabo CPT. V predavanju bo prikazana metodologija, s katero je mogoče simulirati mehaniko likvifakcije s pomočjo preglednic v programu Excel, ki bodo dostopne tudi za prenos.

INTRODUCTION

Liquefaction is a condition in which transient excess pore pressures cause soil to loose stiffness and, possibly, strength. Liquefaction can be triggered statically (slope steepening, over-loading, or rising groundwater pressure) or dynamically (commonly earthquakes, but also machine vibrations and cyclic loading in general). Liquefaction is an undrained phenomenon, where the rate of excess pore pressure generation is markedly quicker than the time required to dissipate those pore pressures by drainage. The drainage aspects are standard geotechnical understanding, with the interesting challenge being in understanding how/why excess pore pressures can develop so quickly.

In the case of static liquefaction with substantial strength loss, various “explanations” have been suggested over the last 100 years generally involving the idea of “metastable grain arrangements”. This idea about the micromechanical behaviour of sand underlies the current liquefaction concepts of a ‘collapse surface’ or ‘instability locus’ (IL), similar frameworks suggesting that there is a limiting frictional strength that can be mobilized before liquefaction (e.g. Lade & Pradel, 1990; Ishihara, 1993; Chu & Leong, 2002).

a) conventional view of load controlled undrained triaxial test data

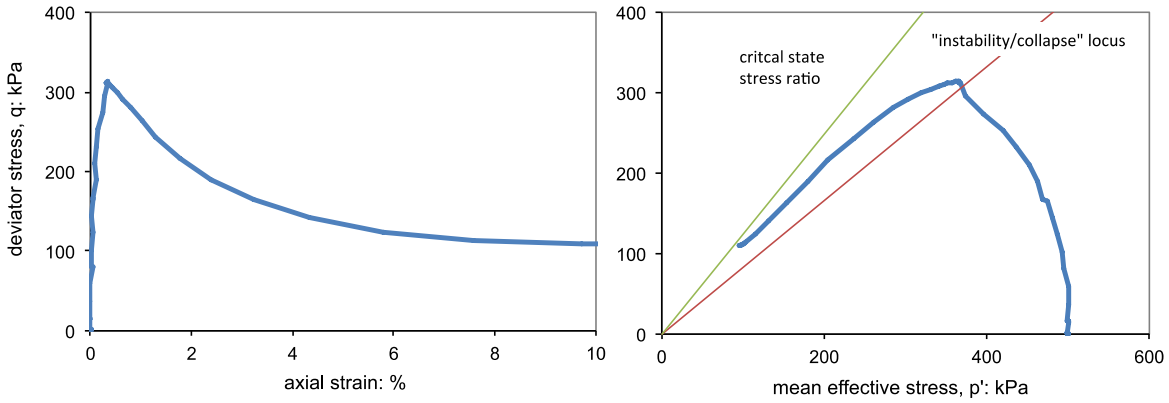

b) same data as plotted as mobilized stress ratio η

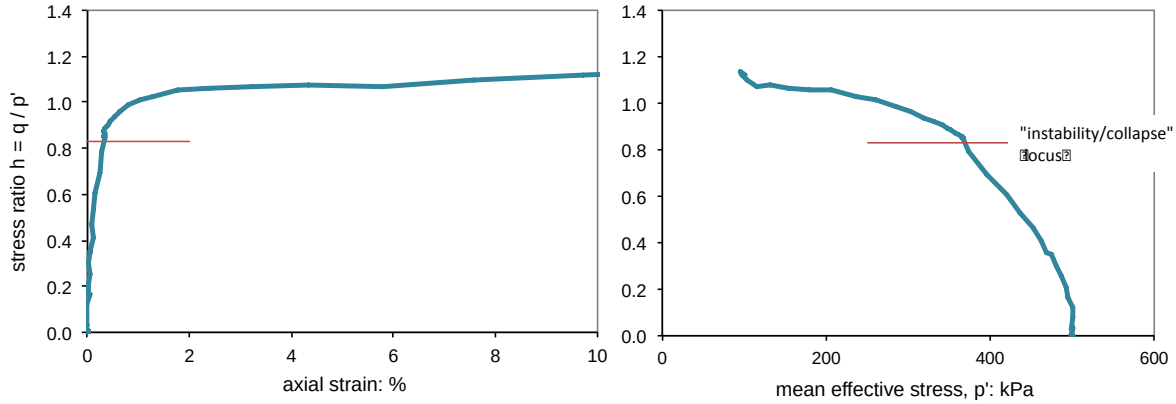

Figure 1. Data showing nature of static liquefaction and the representation of such behaviour with a ‘collapse’ or ‘instability’ locus (Erksak sand, test L601)

The basic flaw in this now widely held 'instability locus' (IL) view as the cause of soil liquefaction is shown on Figure 1. Figure 1a shows an uncontroversial laboratory test with extreme static liquefaction. Figure 1b shows the same data but now viewed in terms of the mobilized stress ratio $\eta=q/p'$, where p´ is mean effective stress and q is deviator stress. The soil shows no significant inflection or other behaviour change at "collapse" when viewed in terms of η and further the soil readily moves to a markedly larger η than existed at "collapse". The hypothesis of a meta-stable arrangement of soil particles cannot be reconciled with measured trends in the mobilized frictional strength of liquefying soil.

In the case of cyclic loading, excess pore pressure caused by 'shakedown' of the soil particles is a far clearer hypothesis and entirely consistent with both the particulate nature of soils and everyday experience in compacting them. If those excess pore pressures lead to static liquefaction, then we return to the understanding just discussed. But, if those pore pressures only cause softening then that is easy to understand since soil stiffness depends on effective confining stress. The challenge with cyclic loading is to define the boundary between "loss of stiffness" and "loss of strength"; which comes down to understanding the nature of static liquefaction and the conditions under which it can arise.

Since soil undergoing static liquefaction still has a stress-strain curve, albeit a brittle one, it is self-evident that liquefaction must be a constitutive behaviour of soil. True understanding starts from this premise rather than invoking geological ideas of metastable grain arrangements. However, the constitutive understanding of soils has been slow to develop with the all the needed factors only falling into place from about 1990 and arguably a consensus only arising about five years ago. Nevertheless, the underlying framework is a line of development within theoretical soil mechanics that traces back to 1885; where we are today builds on a century of developments and has not come "out of the blue" as some sudden new insight.

This paper traces the historical understanding of soil behaviour leading to the generalized critical state soil model *NorSand*, a model that accurately captures the details of soil liquefaction using conventional soil properties and explains why and how liquefaction develops using standard mechanics (and specifically avoiding a collapse surface). Going further, it is necessary to relate what is observed in a laboratory test to conditions in the ground – and that requirement leads to the CPT. This paper therefore puts the understanding gained from *NorSand* into the context of processing CPT data to assess whether a site is potentially vulnerable to static liquefaction.

Although the name *NorSand* might suggest the framework applies to sands, that is incorrect – the mathematics and physics used have no limitation on soil grain size, only assuming that the soil is 'particulate' (i.e. without bonds or true cohesion). NorSand's demonstrated range of applicability is presently from coarse sands to pure silts, including sandy silt till-like soils; examples of calibration and use in silts will be presented.

HISTORICAL BACKGROUND

Soil liquefaction has been a concern to civil engineers for more than 100 years. The Netherlands has long been concerned with natural flowslides, as tidally triggered foreshore slides threated the integrity of the dykes protecting the country from flooding; some 229 slides occurred in the period 1881−1946 (Koppejan et al, 1948). The failure of hydraulic fill dams was a concern in North America over a similar period. Hydraulic filling was a convenient construction method before the availability of the high-capacity earthmoving equipment we know today – the method was essentially to slurry the dam fill in the borrow pit and then pump it to the dam location, where it was discharged. Discharge was from both the upstream and downstream edges of the dam with natural segregation of the pumped slurry producing sand 'shells' to the dam and silty/clay core; Figure 2 shows a section and a photograph of this construction method from 1912. A difficulty with hydraulic fill construction was that there was a tendency of the dams to fail. Calaveras Dam, constructed to 64 m high, suffered a flow failure near the end of its construction in 1918; the failure was described in two articles in Engineering New Record (Hazen and Metcalf, 1918; Hazen, 1918) and a paper in the Transactions of the ASCE (Hazen, 1920). The Discussion that accompanies the Transaction paper is illuminating, and it appears that several other dams failed similarly to Calaveras to

the extent that reading the ENR articles today leaves a clear impression that American civil engineers were aware of liquefaction – indeed, some of the language in 1918 is strikingly modern. Certainly, awareness of liquefaction developed to the extent that the Franklin Falls dam was designed to resist liquefaction – in 1935– and was constructed over the following four years.

The strength testing for Franklin Falls dam (Figure 3) was a milestone for theoretical soil mechanics, as it produced the concept of critical void ratio that now underlies every good model of soil constitutive behaviour. Liquefaction and constitutive modelling are naturally interrelated. Let us now turn to those theoretical developments.

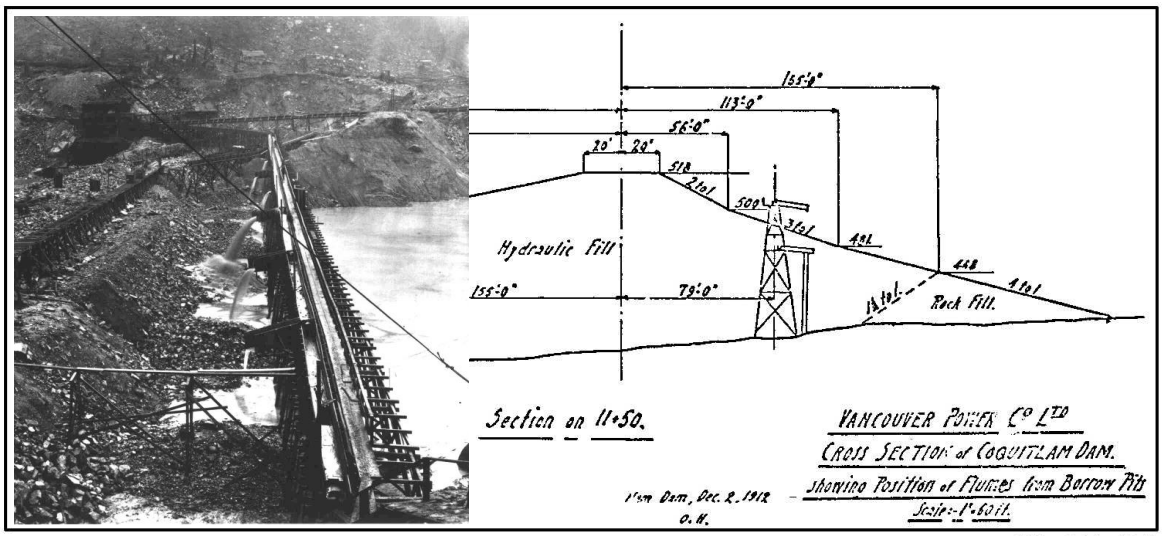

Figure 2. Hydraulic fill construction at Coquitlam Dam in 1912

Figure 3. Franklin Falls dam (NH) – 1936 and the start of critical state theory

DEVELOPMENTS IN THEORETICAL SOIL MECHANICS

Soil has two behaviours that are immediately apparent: plasticity and density dependence. Plasticity because deformations imposed on soil are largely irrecoverable. Density dependence because soil can exist over a range of densities at constant stress, and dense soil behaves quite differently from loose soil.

Most soil models are based on plasticity, which is a macro-scale abstraction of the underlying grain realignments and movements. Plasticity is the idea that some (and usually most) strains are not recovered when a body is unloaded, an idea which dates back 150 years. Tresca (1864) first proposed a yield condition which distinguished between those stress combinations that cause yield (or irrecoverable strains) from those that do not (elastic strains). During yielding, strains are viewed as comprising two mechanisms, one elastic (denoted by the superscript "*e*"), and one plastic (denoted by the superscript "*p*"), with the relation:

$$\varepsilon = \varepsilon^e + \varepsilon^p \qquad [1]$$

Equation [1] underlies every good model for soil behaviour.

Soil is commonly idealized as a collection of near spherical particles. If the particles are rigid, then deformation can only take place if the packing of the particles changes – thus dilation is a fundamental and intrinsic behaviour we expect in any soil. This theoretical expectation was established by Reynolds (1885). Although the term 'dilation' (also called 'dilatancy') is sometimes used to mean volumetric strain (ε_v), applied mechanics uses dilation *D* as the ratio of volumetric strain increment to distortional strain increment:

$$D = \Delta\varepsilon_v / \Delta\varepsilon_q \qquad [2]$$

… where for triaxial compression $\Delta\varepsilon_q = 2\,(\Delta\varepsilon_1 - \Delta\varepsilon_3)/3$. This strain invariant $\Delta\varepsilon_q$ generalizes to 3D (Resende & Martin, 1975; Jefferies & Shuttle, 2002) although as a less familiar equation.

If the soil is loose 'dilation' will involve a reduction in soil volume; this was understood early in the 20th century to be a mechanism for causing excess pore pressure in soils if the loading was undrained (and resulted in the testing for the Franklin Falls dam mentioned earlier). Given that dense soil increases in volume during shear while loose soil contracts, it is natural to wonder how the two behaviours are related. Casagrande (1936) used a shear box tests to test the proposed fill for Franklin Falls dam. It was found that loose sands contracted and dense sands dilated until approximately the same void ratio was attained at large strains as shown on Figure 4. This large strain void ratio distinguished which mode of behaviour the soil exhibited, and in particular anything looser was always contractive. Casagrande termed the void ratio that demarked contractive versus expansive volumetric strain behaviour as the *critical void ratio.*

Shortly after the testing at Franklin Falls dam, part of Fort Peck dam failed in a flowslide. Subsequent testing of sand from this dam lead to the understanding that the critical void ratio depended on confining stress (Taylor, 1948) with a unique relationship – what we know today as the *critical state locus* (CSL). Getting slightly ahead of history, the uniqueness of the CSL has been disputed by various workers since then but invariably that has come down to workers misunderstanding the physics. The critical state involves two conditions: zero dilation (D=0) and zero change of dilation with further shear ($\Delta D/\Delta\varepsilon_q$ =0). Both conditions must be met for the soil to be at the critical state. The various issues around uniqueness of the CSL were comprehensively investigated by Been et al (1991) and with uniqueness of the CSL confirmed.

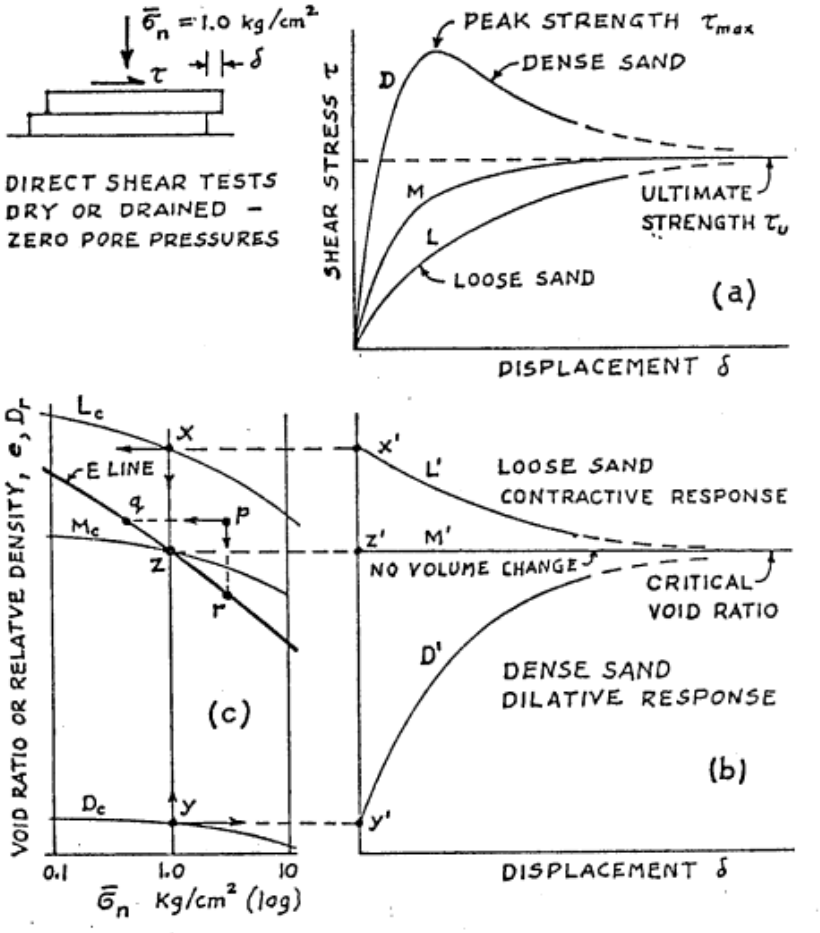

Figure 4. Critical void ratio defined by Casagrande (1935)

The CSL is often idealized as semi-log relationship between critical void ratio e_c and mean effective stress p', although soils when tested tend to deviate from this idealization. Figure 5 shows an example of a CSL for a sandy silt together with the best-fit idealization to the test data. Also shown on this figure is the usual idealized CSL, optimized over the stress range of engineering interest, with the form:

$$e_c = \Gamma - \lambda_{10} \log (p') \qquad [3]$$

… where Γ, λ_{10} are soil properties (or at least properties within the engineering judgment used to idealize this behaviour). There is no theoretical difficulty is using better fits to the data, with some workers preferring 'power law' idealizations. The notation λ_{10} is used to remind that the property is related to base 10 logarithms, the most familiar way of looking at data. Constitutive models tend to use natural logarithms with the corresponding soil property λ where $\lambda = \lambda_{10}/2.3$.

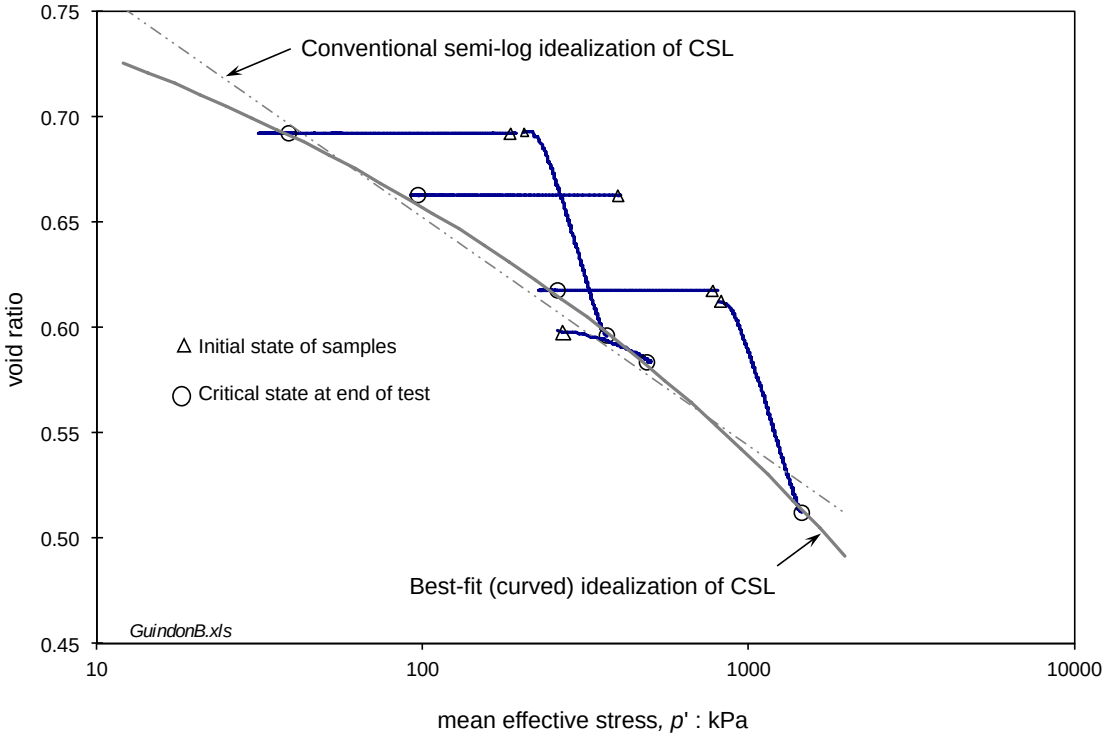

Figure 5. Examples of CSLs for a sandy silt

Dilatancy of soils was known from Casagrande's early shear box experiments. A school of thought then developed that the soil behaviour should be understood in terms of friction angles (viewed as the fundamental soil "property") corrected for the work transferred by dilation. Taylor (1948) was a principal proponent of this view, although its first formal statement as an equation appears to be Bishop (1950). Adopting Bishop's concept, but changing from his use of friction and dilation angles to stress and stain invariants, gives a general form of soil strength:

$$\eta_{max} = M - (1-N)\, D_{min} \qquad [4]$$

… where η_{max} is the soil strength (analogous with peak friction angle) and D_{min} is the minimum dilatancy (minimum because of the compression positive convention of soil mechanics and analogous to peak dilation angle). M is the critical friction ratio and N is a volumetric coupling parameter (after Nova, 1982). Both M, N, are soil properties and are independent of void ratio and mean effective stress; by convention they are determined under triaxial compression conditions (with the subscript '*tc*' being used to denote this). Figure 6 shows a set of drained triaxial compression tests over a wide range of stress levels and sand density illustrating the trends found in soil behaviour and the meaning of these two soil properties.

Equation [4] is widely used to represent soil behaviour and is not associated with any particular constitutive model – it simply captures the way all soils behave, from gravels to clays and with the suggestion that the equation even extends to rockfill. The only difference from one soil to another is the numerical values of M, N, properties which are affected by particle shape and mineralogy.

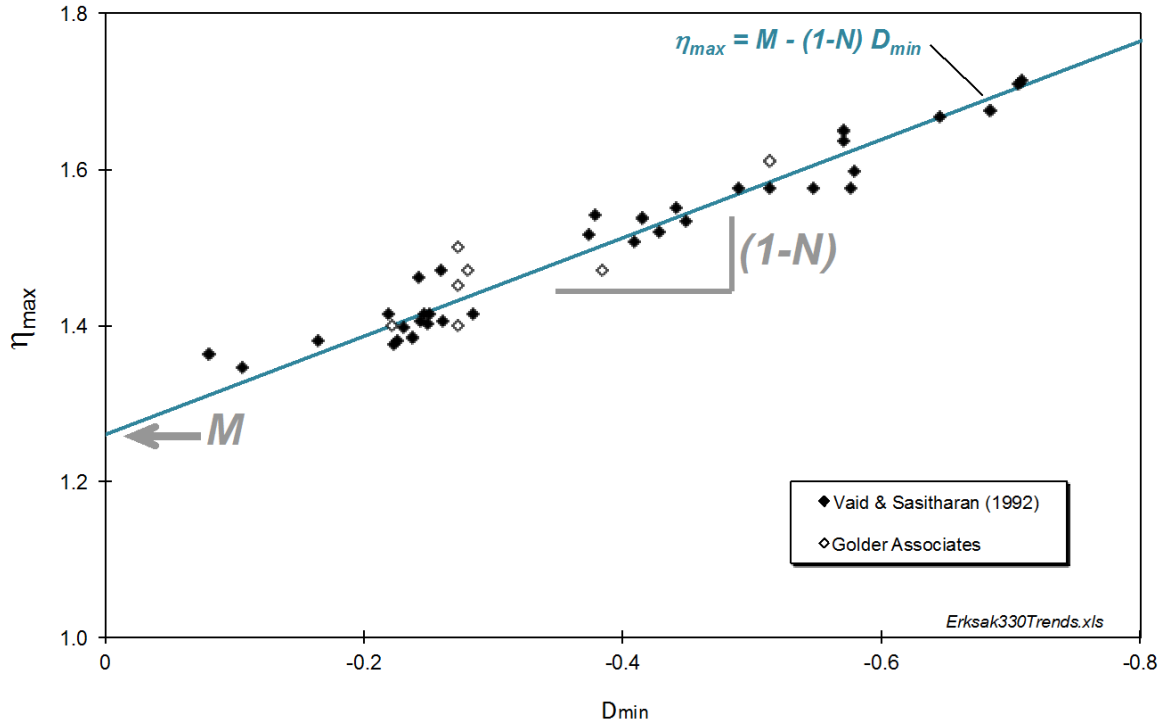

Figure 6. Data showing the drained triaxial compression strength of Erksak sand (test by two laboratories, a range of initial sample densities and confining stress)

Equation [4] is about "strength". However, dilation exists throughout the entire stress-strain behaviour. Recognition of this fact led to the framework often referred to as stress-dilatancy theory (Rowe, 1962) where 'strength' is generalized to mobilized stress ratio (η=q/p) in terms of current dilation:

$$\eta = M_i - D^p \qquad [5]$$

… where M_i is an evolving coefficient (related to the soil property M_{tc}).

When Rowe developed stress-dilatancy theory there was an implicit hope that M_i might be related to the mineral-mineral sliding fiction of the soil particles: $M\mu$. That idea turns out to be a lower bound to data, with the 'operating' coefficient in equation [5] evolving with strain within the restriction $M\mu < M_i < M$. The difficulty that then followed was a lack of guidance on how M_i should evolve, not rectified until nearly forty years later by Dafalias and co-workers (Manzari & Dafalias, 1997; Li et al, 1999). Notice that D^p in [5] is the ratio of plastic strain increments, necessary because stress-dilatancy is about "work" while elasticity is about "energy storage".

One of the differences between plasticity and elasticity is the treatment of strains. In elasticity, principal strain increments are in the same direction as principal stress increments. But, in plasticity, strain increments depend on the stresses not the stress increments.

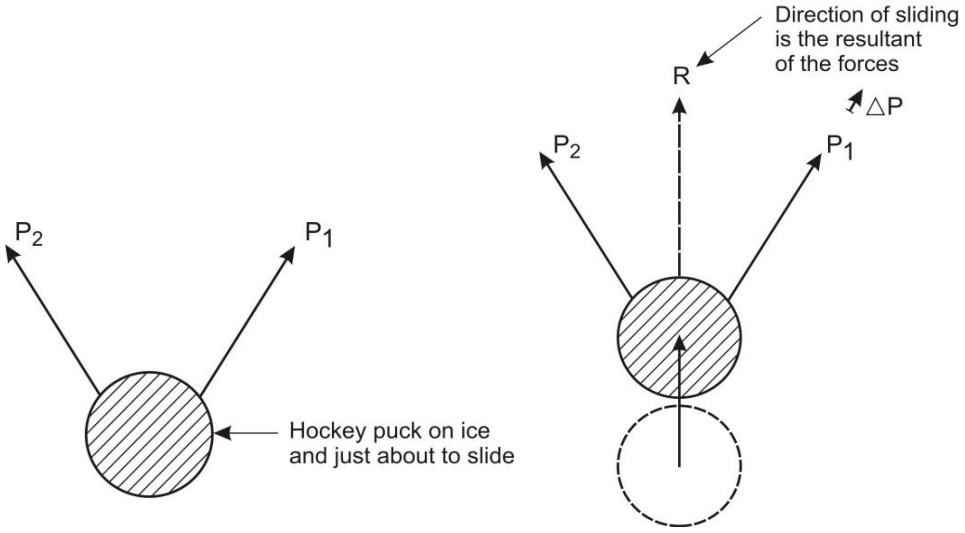

Figure 7. Illustration of normality by hockey puck analogy

A simple thought experiment to show the direction of plastic strains is shown in Figure 7. An ice hockey puck is sitting on the ice and is about to slide under the action of two forces, both of which are applied by strings acting at an angle. Sliding starts when the force on one string is increased slightly. One can immediately appreciate that the puck starts moving in the direction of the force resultant, not the force increment that initiated sliding. This is the simplest explanation of what is termed the *normality* principal or, alternatively, *associated flow*. Plastic strain increments are directed normal to the stresses defining the yield surface as illustrated on Figure 8, not to the stress increment that initiates the yielding. Normality was given further impetus by Drucker (1951) who cast the principle in terms of the Second Law of thermodynamics – normality is fundamental, not an idealization.

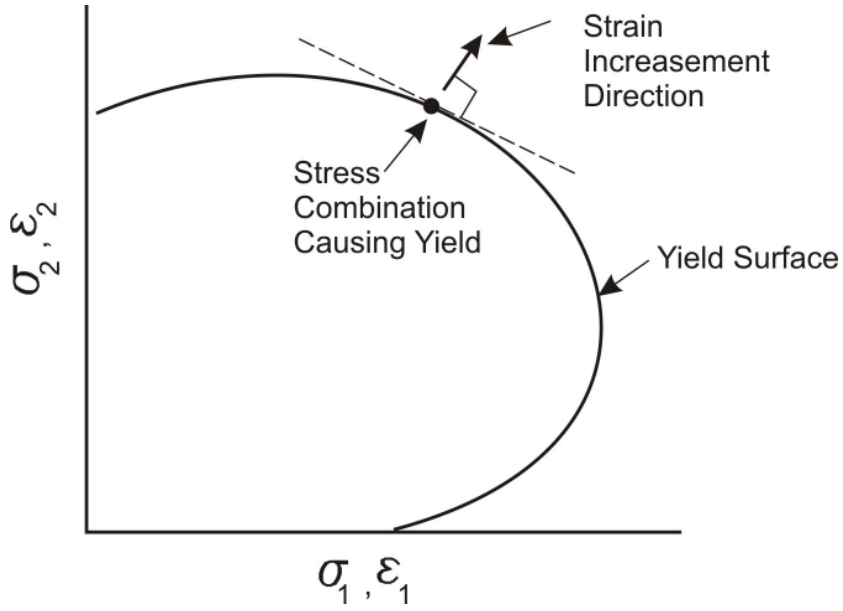

Figure 8. Definition of normality (associated plastic flow)

Drucker et al. (1957) showed that the correct way to apply plasticity to soil behaviour was by recognizing that Mohr-Coulomb criteria is a limiting stress ratio and not a yield surface. Rather, the yield surface must

intersect the normal compression locus (NCL), since normal compression produces irrecoverable strains. Hence, the spectrum of soil density states (conventionally called consolidation theory) was intrinsically coupled to soil constitutive behaviour, because the yield surface size was coupled to the stress, causing yield in isotropic compression. This isotropic yield stress would conventionally be recognized as the preconsolidation pressure, and there is considerable existing experience as to how preconsolidation varies with the void ratio of soils. Although constitutive models can be developed using the preconsolidation pressure, the CSL also provides a relation between void ratio and stress. The CSL is a more natural basis for the hardening law as the critical state involves shear strain and, by definition, a zero dilation rate. In effect, the critical state is the same thing as the Taylor/Bishop energy corrected friction angle concept.

These ideas of critical friction and correctly associated yield surfaces were pulled together by various people at Cambridge University (Roscoe, Schofield and Thurairajah, 1963; Roscoe and Burland, 1968; Schofield and Wroth, 1968) to produce a predictive constitutive framework known as critical state soil mechanics, or CSSM. Figure 9 shows the key idealizations of Original Cam Clay schematically.

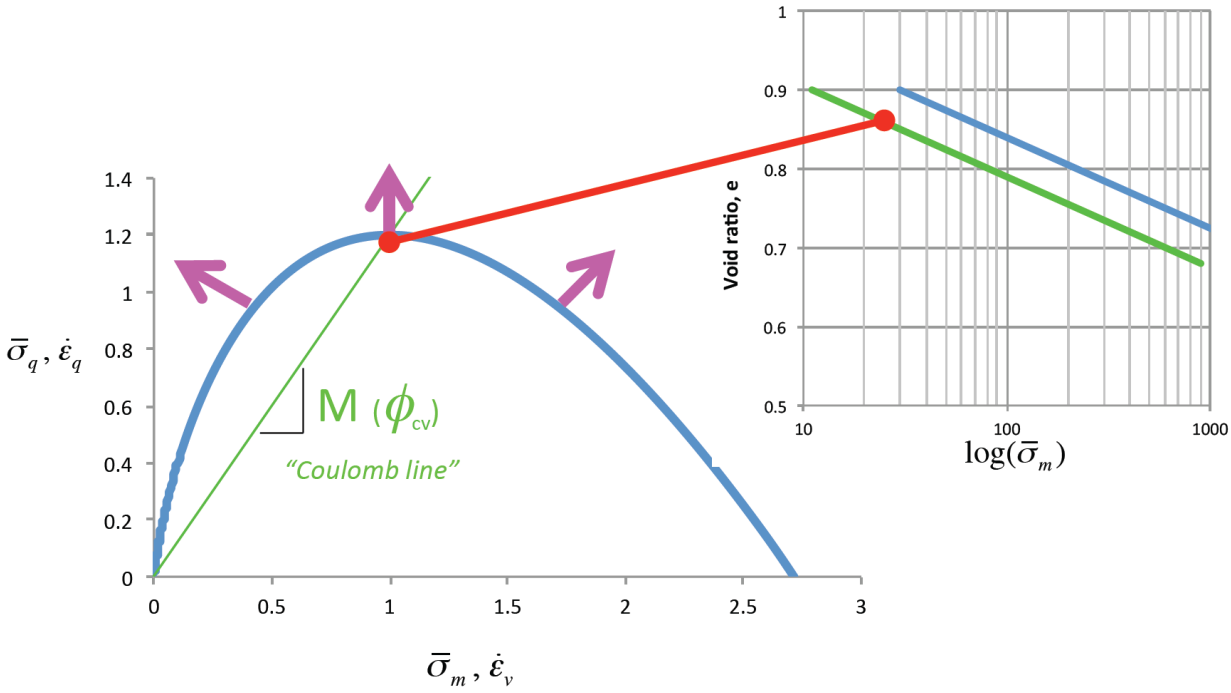

Figure 9. Original Cam Clay in one picture. The left hand plot shows the yield surface (blue) with plastic strain increment vectors (pink) normal to the yield surface. The right hand plot shows e-log(p) with CSL in green. The points linked in red are common to both plots – as void ratio changes, so does the size of the yield surface.

The theory of critical state soil mechanics (CSSM) is a widely taught model for soil behaviour, and by a considerable margin. CSSM links void ratio, mean stress, and shear stress in a single mathematical framework, providing a complete, self-contained, and thorough model that is the end result of about 100 years of theoretical developments. But, despite these attractions, the well-known variants of Cam Clay (Schofield & Wroth, 1968) and Modified Cam Clay (Roscoe & Burland, 1968) are avoided in modelling most real soils, including sands and silts, because of their inability to dilate and yield anything like real soils (Mroz and Norris, 1982).

Figure 10 illustrates the fundamental problem of Cam Clay with dense soils. Figure 10a shows the state-path of a moderately dense sand sample tested in drained triaxial compression; Figure 10b compares the measured stress-strain curve with that predicted by Cam Clay. It is not a matter of "accuracy" with

perfectly simple laboratory test on a readily prepared sample having strengths predicted by Cam Clay that are orders of magnitude larger than measured.

Clearly, something fundamental has been missed with Cam Clay. All a bit surprising from a train of formal theoretical developments – could 'the math' be that wrong? It was full-scale construction experience that resulted in the understanding of where CSSM has gone "wrong".

a) Measured state path

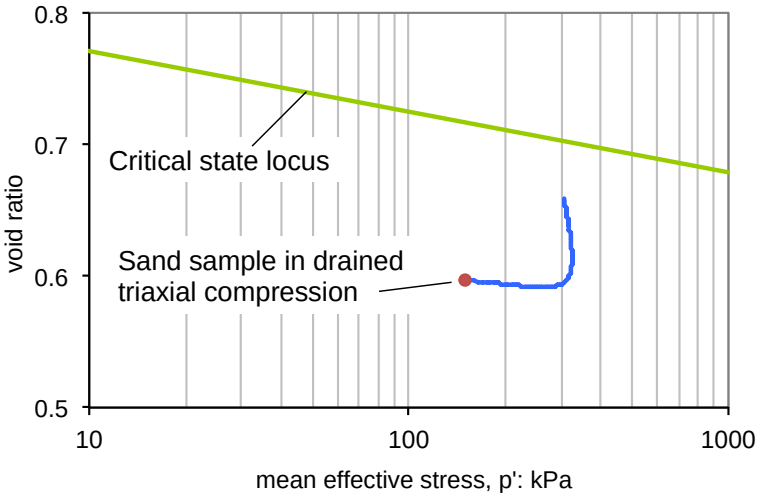

b) Predicted versus measured stress-strain behaviour

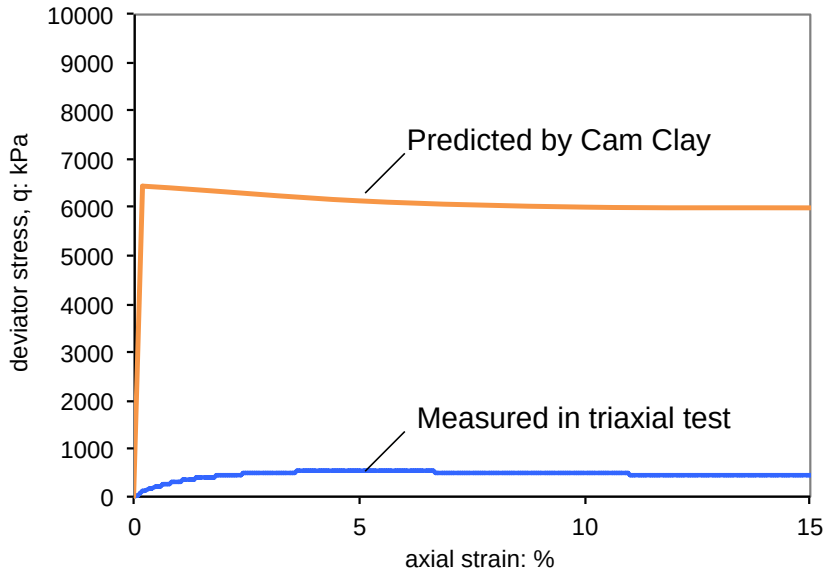

Figure 10. The basic problem with Cam Clay

SAND BEHAVIOUR IN HYDRAULIC FILLING

Substantial reserves of oil exist in the Canadian Beaufort Shelf, with considerable exploration during the 1980's. This region is ice covered for about nine months of each year and, depending on location, that ice can move. Moving ice causes large horizontal forces on offshore structures. Because of these forces, oil companies exploring the area using artificial islands for the exploration drilling, with the islands having sufficient mass to resist ice forces. Islands were constructed using hydraulically placed sand in the open-water of the summer months with exploration drilling during the following winter. Simple islands were satisfactory for near-shore exploration, but as drilling moved further offshore the increasing water depth made islands difficult to construct in a single open-water season because of rapidly increasing fill volumes. All of the oil companies therefore adopted variations of caisson-retained islands where a structure minimized the fill volume while retaining sufficient mass to resist forces from moving ice. Figure 11 shows one such structure, the Gulf Canada Resources drilling barge "Molikpaq". A berm was used beneath the Molikpaq so that the constant set-down depth of the Molikpaq could accommodate a range of water depths. Figure 12 shows a section through the berm and structure.

Figure 11. Molikpaq Arctic drilling platform in moving ice

The berm and core were both constructed from hydraulically placed clean sand. This sand was pluviated through water and without any mechanical compaction or preloading: geologically, the ideal situation for *normally consolidated* soil. Figure 13 illustrates sand deposition into the berm by bottom discharge from a dredge.

The nature of oil exploration in the Arctic offshore was such that considerable effort was put into construction quality assurance. In the case of the Molikpaq core and berm, CPT soundings were used to verify fill adequacy. The number of CPT soundings varied from site to site (the Molikpaq was eventually deployed at five locations), but typically 15 CPT in the berm before platform set-down followed by a further 30 CPT through the core and berm once the platform was fully deployed. Since the core occupied an area of just 72m x 72m these CPT comprise an unusually comprehensive investigation of trends in fill variability with location and depth.

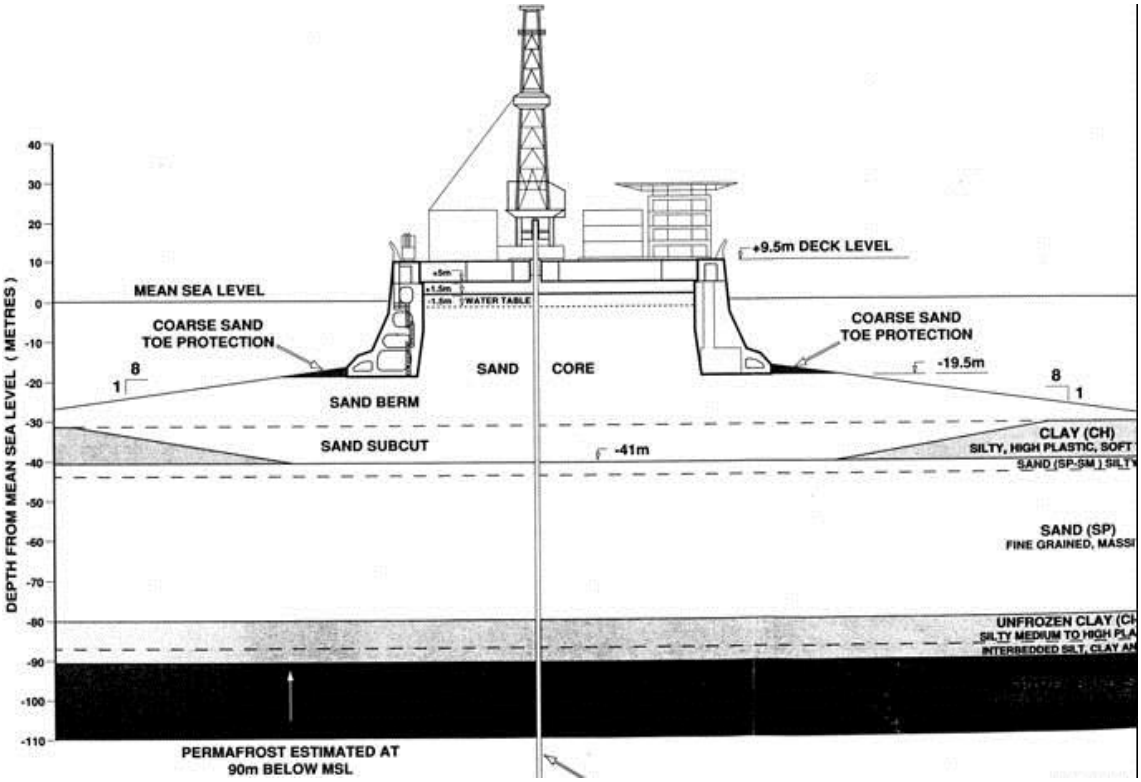

Figure 12. Cross-section Molikpaq show sandfill core and berm

Figure 13. Hydraulic placement of sandfill into Molikpaq berm – 5000 m3 placed by pluviation through water (bottom-valve discharge) in ten minutes

There is a direct relationship between CPT tip resistance (q_t), confining stress, and relative density (D_r). The relationship has been found for about ten sands, and is sand-specific with sand compressibility affecting the relationship from one sand to another although the basic q_t-p'-D_r pattern remains the same.

Figure 14 shows the results of CPT testing on a Molikpaq berm transformed into distributions of relative density (D_r) at various stress levels (depths from top of berm). Notice that 'loose pockets' remain as 'loose pockets', and similarly for dense zones, as stress levels increase. Figure 15 shows the same data now transformed into a familiar e-log(p') plot; there is a bandwidth with probability for a particular void ratio.

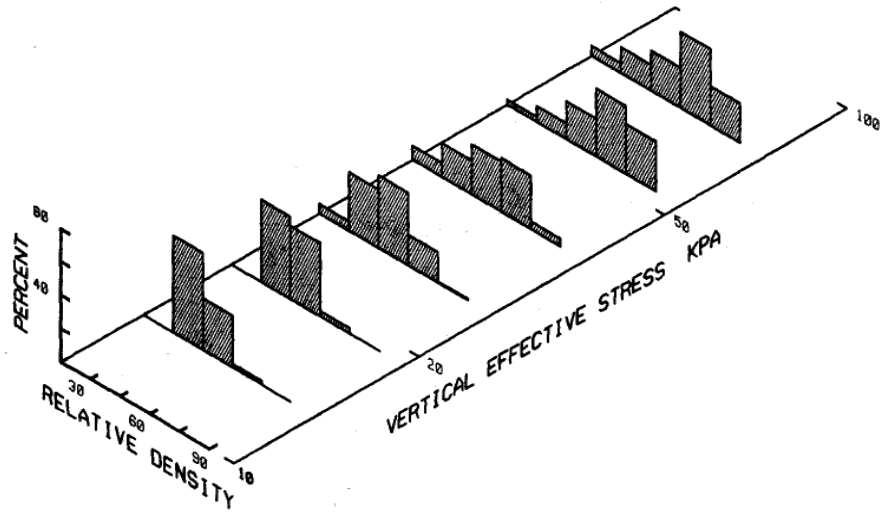

Figure 14. Distribution of fill density in hydraulic sand fill berm constructed as shown in Figure 13 (Stewart et al., 1983)

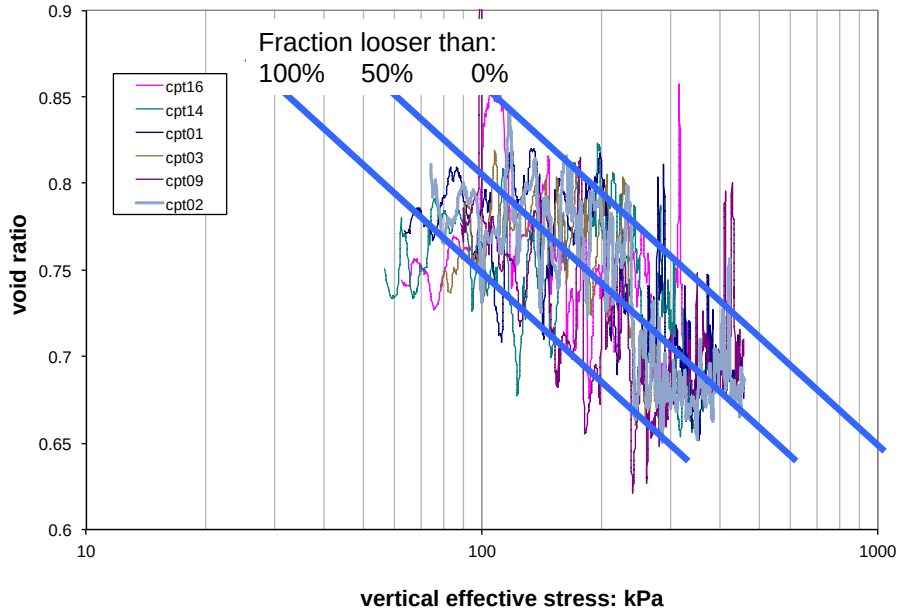

Figure 15. CPT data in berm transformed into void ratio profiles and with probability limits indicated as blue trend lines

The key insight from Figure 15 is that there is no single normal compression locus (NCL). Recall, that the construction of this fill was pluviation through water without compaction or the like. When this observation was reported (Stewart et al, 1983) it was thought to be a new finding. It was subsequently discovered that Ishihara et al (1975) had inferred exactly this concept of non-unique NCL from laboratory testing. Further

experimental work explicitly confirmed the existence of non-unique NCL (belatedly reported by Jefferies & Been, 2000).

STATE PARAMETER

The existence of a band of NCL's (mathematically "an infinity") is not a detail, but is the underlying cause of what is "wrong" in Cam Clay. The situation is illustrated on Figure 16. The left hand picture shows the Cam Clay view (with a curved CSL to highlight that the idealization of the CSL is not the issue). Cam Clay a unique NCL that is parallel to the CSL and separated from it by the spacing ratio (r=2.7 for Original Cam Clay, r=2.0 for Modified Cam Clay). Dense states, as illustrated, imply large OCR. The right hand picture shows the real behaviour of sand, with an infinite number of NCL. Now, recall that the basic idealization of plasticity theory for soil requires the yield surface to intersect the – self-evidently, it is not possible to have a single yield surface for a particular void ratio that both intersects the CSL and all the NCL's. The solution to this situation is to recognize that each NCL represents a different yield surface and to characterize that situation – with the simplest and most fundamental characterization being to rely on the CSL as being unique and to measure from that: thus, the state parameter ψ as shown on Figure 16.

a) "Conventional" soil mechanics *b) Actual soil behaviour*

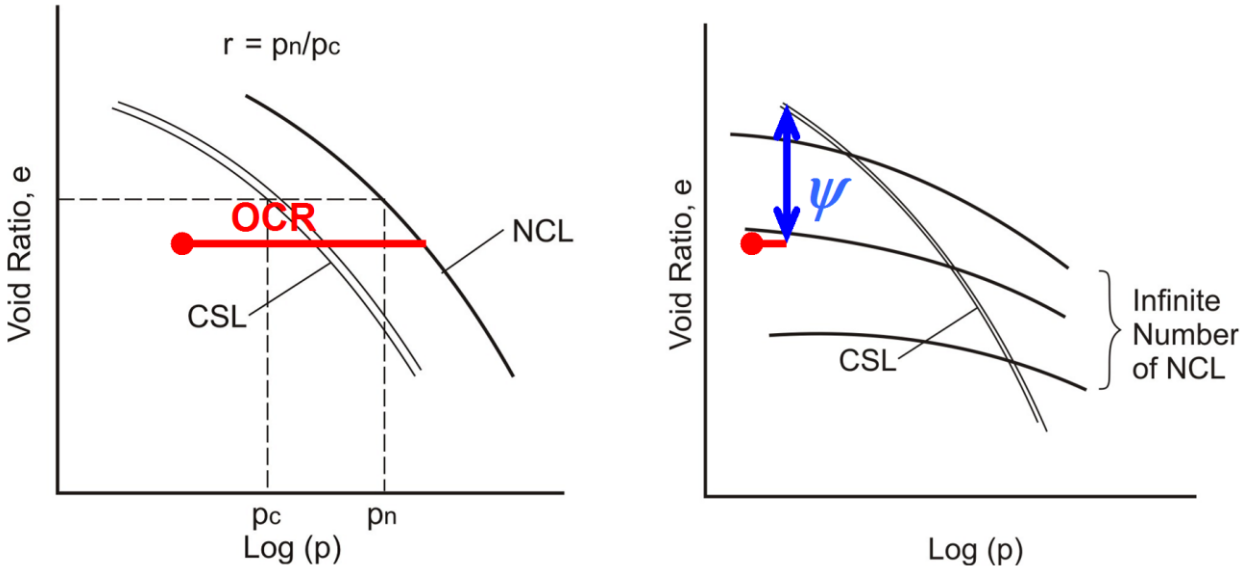

Figure 16. Implications of non-unique NCL for characterization of soil state and showing definition of the state parameter ψ

Any soil is now characterized by two state measures: OCR, which describes how close the soil is to its yield surface; and, ψ which describes where the yield surface currently lies compared to the soil's current critical state. An obvious expectation of using ψ to characterizing soils is that soil strength will be unified (which is not achieved by relative density or void ratio). Characterization using ψ will certainly be independent of stress level, but likely also of other aspects including fines content and the like since those aspects control the CSL. This was the proposition of Been & Jefferies (1985), supported by considering the drained frictional strength of sands ϕ over a range of initial densities, confining stress and silt contents. An expanded version of the Been & Jefferies data summary is shown on Figure 17, this figure including some 240 drained triaxial compression tests on various sands. Soil gradation is shown using the notation D_{50}/fines; thus "Alaska 240/10" has a median grain diameter D_{50} = 240 microns and a fines content (faction silt sized and finer) of 10%. A simple linear trend is apparent between ϕ and ψ_o with a fairly narrow bandwidth for all the test data. Expectations anchored in theoretical plasticity produce a simple, usable soil strength characterization that is substantially independent of soil geology.

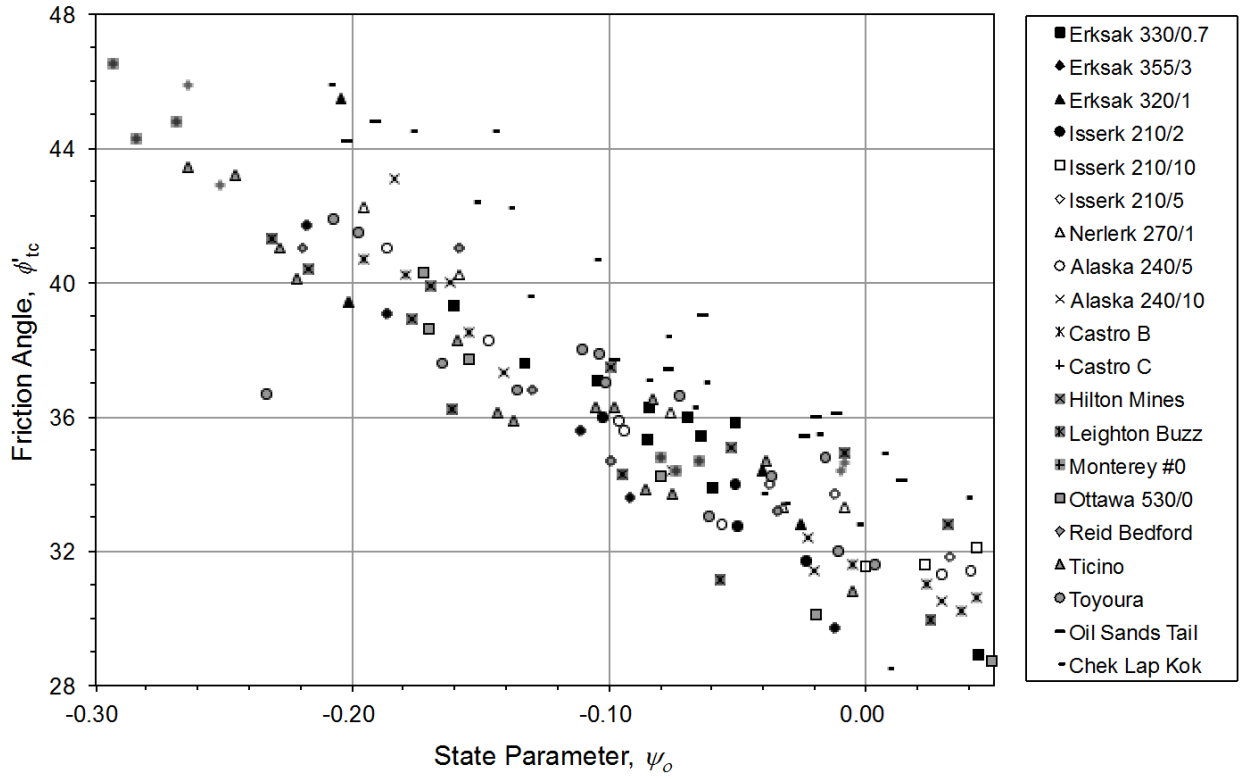

Figure 17. Soil frictional strength as a function of the state parameter (after Been & Jefferies, 1985, updated with additional data)

This idea that the trend between ϕ and ψ_o was independent of soil geology has been overtaken as the state parameter approach has moved from sands to till-like soils and to pure silts. Broadly, well-graded soils have less free void space and correspondingly show a greater sensitivity to the effect of volumetric strain while silts do the opposite. Giving the state parameter even wider applicability has involved introducing one further soil property in a *state-dilatancy* law (analogous to stress-dilatancy) that is defined as:

$$D_{\min} = \chi_{tc} \psi \qquad [6]$$

...where χ_{tc} is a soil property defined under drained triaxial compression.

Note that ψ is defined as its current, not initial, value in equation [6]. We also observe that D_{min} generally occurs at the peak stress ratio. D_{min} is preferred to strength as D_{min} is related to the change in void ratio and has void ratio as its input, essentially the same quantity is used on both sides of equation [6]; it also recalls back to Reynolds (1885) who showed that dilation is a kinematic consequence for deformation of particulate materials. It is all a matter of particle geometry and their ability to move; stress change is the consequence, not the input. Using the current value of ψ means that there is no offset (or constant) in [6] and the condition ψ = 0 naturally gives D_{min} = 0, which is the critical state. Figure 18 shows data on a single sand showing the limited scatter found with this state-dilatancy approach.

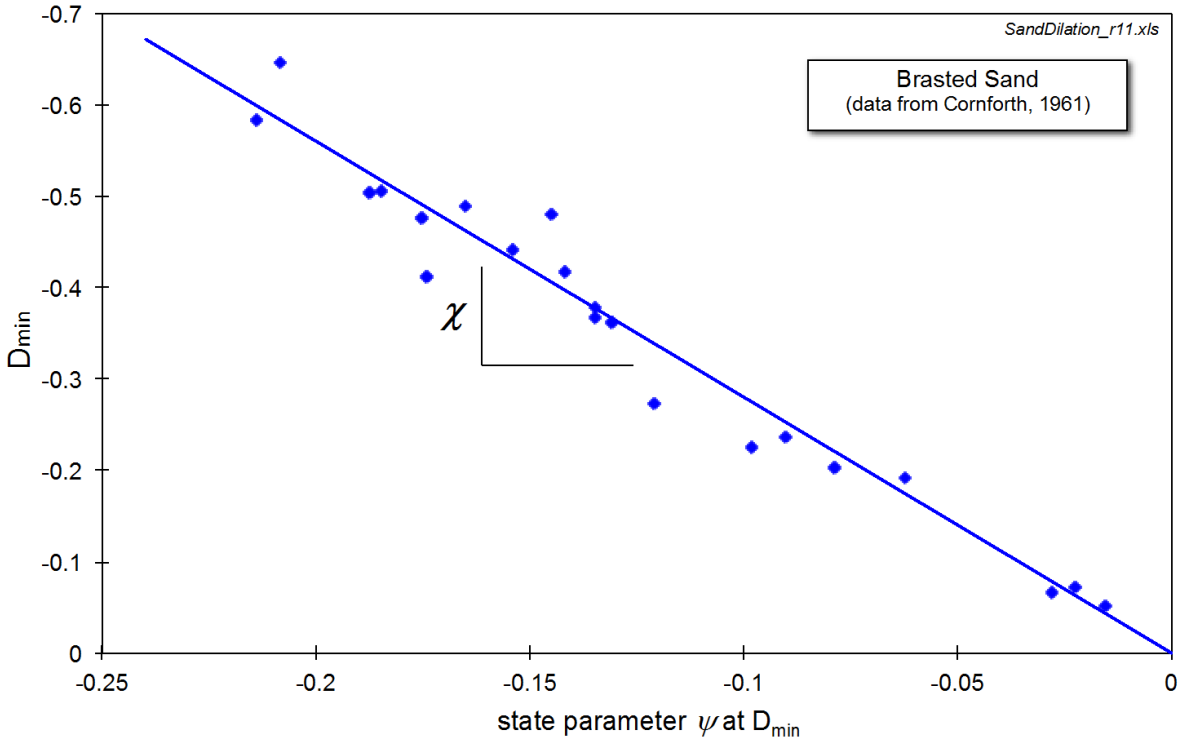

Figure 18. Test data showing nature of state-dilatancy and the definition of the soil property χ

The proposition of Been & Jefferies (1985) amounts to a common χ_{tc}~ 4 for uniform sands with trace to some silt. Subsequent testing has found that tills tend to double this value while pure silts seem about half. Accepting that a soil property is involved improves the available precision from the state parameter approach, although we have added a little bit of complexity in processing laboratory test data to gain a simple and elegant framework.

NORSAND

The state parameter has been outlined as characterizing soil behaviour, and it is usable as that. However, the real power behind the state parameter comes when it is incorporated within constitutive models, as it leads to models that predict the entire spectrum of soil behaviour using the few soil properties just discussed (themselves independent of void ratio and stress level). There are several models now available based on the state parameter, with the differences between them being in the nature of modelling details and/or mathematical approach. NorSand was the first of these models (Jefferies, 1993), and is arguably the easiest to understand.

Like all plasticity models, *NorSand* comprises: i) a flow rule giving the ratio of plastic strain increments; ii) a yield surface defining the limit of elastic behaviour; and, iii) a hardening law defining how the yield surface changes size with plastic strain. The complete equation set for the 3D version of *NorSand* (Jefferies & Shuttle, 2002) is given in Appendix A, broken down into these three aspects together with a specification of internal variables. *NorSand* uses the soil properties discussed earlier together – all of which are conventional and determined under triaxial compression - with a single new soil property, the plastic hardening modulus.

NorSand may be best understood by considering its yield surface, and examples of that are shown on Figure 19 for both loose and dense soils. The similarity of NorSand to Original Cam Clay is apparent, which follows because NorSand is a strict implementation of Drucker et al (1957) and thus has the same theoretical idealizations used to derive the yield surface. So where is the difference between the NorSand yield surface and Cam Clay? There are the two key differences.

a) Loose Soil

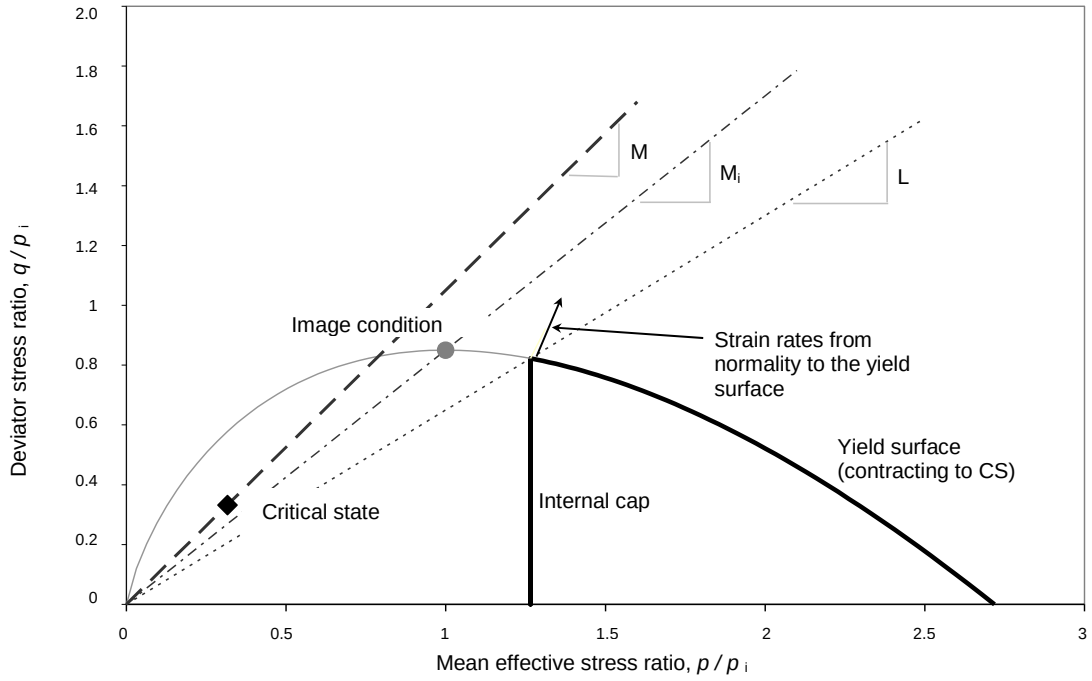

b) Dense Soil

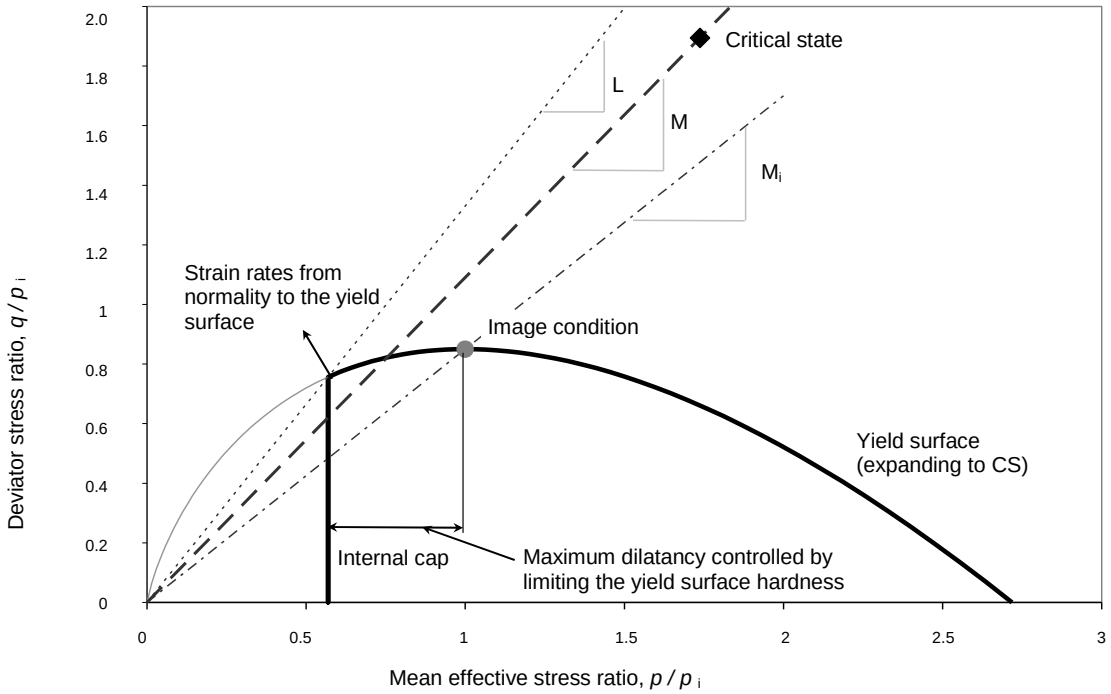

Figure 19. NorSand yield surface, limiting stress ratio η_L and image condition (top: loose soil; bottom: dense soil)

First, *NorSand* does not use the mean effective stress at the critical state p_c to scale the size of the yield surface. Instead NorSand uses another condition, that of the *image state*, and denoted by the subscript *i*. Recall that there are two conditions for the critical state, $D = 0$ and $\dot{D} = 0$. The condition where $D = 0$ alone exists is referred to as an *image* of the critical state since only one of the two conditions for criticality is met. The mean effective stress at the image state, p_i describes the size of the yield surface, but this stress p_i generally does not lie on the CSL; NorSand then invokes the *Second Axiom* of critical state theory: soil moves to the critical state with increasing shear strain. This is most naturally stated as:

$$\psi \to 0 \quad as \quad \varepsilon_q \to \infty \qquad [7]$$

… and which is used to provide the hardening law to move p_i to the CSL with plastic shear strain. The *Second Axiom* never arose in Cam Clay explicitly because it is enforced tacitly through the assumption that all yield surfaces intersected the CSL; Cam Clay assumes the end condition as its starting point. That cannot be done in any generally, so the *Second Axiom* must become the hardening law.

Notice the *Second Axiom* is stated in terms of shear strain because the critical state is a condition of shear. There are conditions of loading at low stress ratios, for example confined geostatic compression, where soil states will move away from the critical state but these paths have limited shear strain and thus do not conflict with the axiom.

Second, NorSand uses an internal "cap" to the yield surface. A key feature of dense soils, whether sands or clays, is that dilatancy is limited to a maximum value for that specific soil state as defined by equation [6]. Conventionally, dilation is limited by invoking a non-associated flow rule with an appropriate choice of dilation angle. That approach is not acceptable within a strict critical state framework because normality is used to derive the yield surface. Instead, realistic maximum dilatancy is controlled through the hardening parameter, p/p_i as shown in Figure 19. The value of p_i is limited with respect to the current stresses, and this then controls the dilatancy through normality. The limit on hardening is given by:

$$\left(\frac{p_i}{p}\right)_{\max} = \exp\left(-\chi_i \psi_i / M_{itc}\right) \qquad [8]$$

The natural form for a hardening law that complies with the Second Axiom, while respecting the constraint on dilatancy, is a simple difference equation:

$$\frac{\dot{p}_i}{\dot{\varepsilon}_q} = H\left(p_{i,\max} - p_i\right) \qquad [9]$$

Equations [8] and [9] are the fundamental difference between *Original Cam Clay* and *NorSand*. These two steps provide realistic yielding, consistent with an infinity of NCL, by decoupling the yield surface from the CSL. Original Cam Clay is recovered as a specific case of NorSand by choosing the initial conditions such that ψ_i=0, which aligns the yield surface with the CSL, and a matching plastic hardening H=1/($\lambda-\kappa$) that keeps the yield surface on the CSL as plastic strains develop.

The full set of the *NorSand* equations are given in Appendix A and, like other comparable models, they can appear intimidating to practical engineers (the formalism of applied mechanics does not aid adoption of the ideas). This situation is further compounded because these models do not give an equation relating stress and strain – instead, the models give the current soil stiffness. Integration is necessary to get stress-strain curves from these models that can be compared with laboratory tests. The nature of these plastic models is that integration must be numerical except in rare special instances. But, for standard laboratory tests (triaxial, simple shear, oedometer), numerical integration is readily done in a spreadsheet using the Euler method and well within practical use:

$$\sigma_{j+1} = \sigma_j + d\sigma_j / d\varepsilon \, \Delta\varepsilon \qquad [10]$$

… where 'j' is the current step and 'j+1' the next step. The Euler method simply steps forward using stiffness computed for the current condition to estimate the next point on the stress-strain curve. This is the oldest numerical method, easily understood, and sufficient for geotechnical modelling. The procedure can be written as:

Loop over…

apply plastic shear strain increment

FLOWRULE: recover all plastic strains increments

HARDENING: use hardening rule to get increment of image stress

NEW STRESS: apply consistency condition to determine new stress state

ELASTICITY: add in elastic strains from stress changes in load step

UPDATE: strains, void ratio, state parameter

Notice in the above procedure that the flowrule and hardening law are both used explicitly, but that the yield surface does not appear directly. That is because the yield surface is implicit in the *consistency condition*, the final step in integrating plasticity models. Work hardening (and softening) plastic models change the size of their yield surface with plastic strain. The *consistency condition* is simply that the stress state must remain on the yield surface during plastic strain, so that the stress state evolves on a one-for-one basis with the evolution of yield surface size. The consistency condition is illustrated in Figure 20, which shows an initial yield surface that has hardened after an increment of plastic strain. In the case of laboratory "element" tests, the stress state is simply computed from the consistency using the known direction of stress increments; however, this is not a single equation as, for example, the situation is different in undrained simple shear compared to drained triaxial compression – thus, there are test-specific versions of the consistency condition. In finite element implementations, the consistency condition drives the plastic yielding solution algorithm.

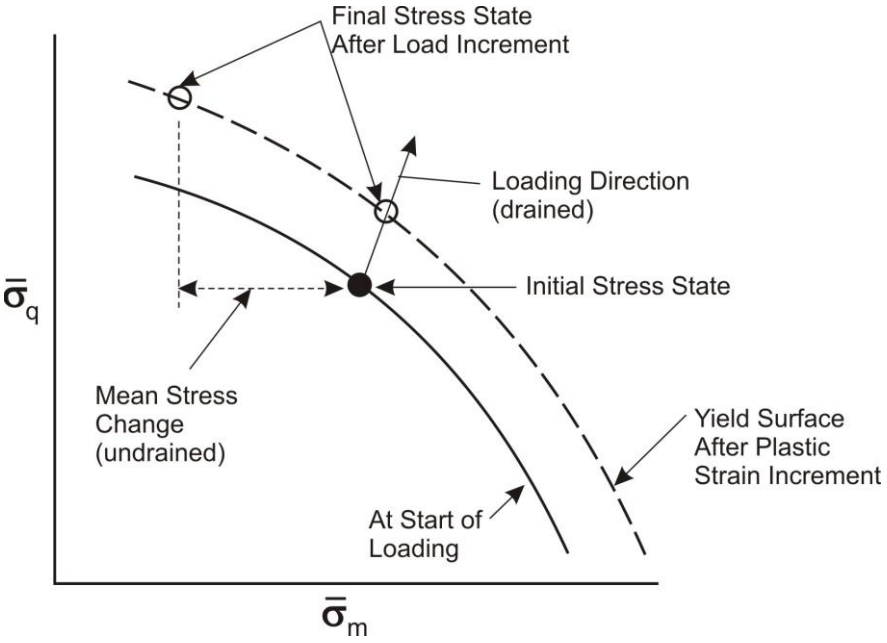

Figure 20. The consistency condition for updating stress during yielding

Figure 21 shows examples of the match between NorSand and test data for a quartz sand in drained triaxial compression. An excellent fit is found, and the soil behaviour nicely responds to the different initial void ratios of these two samples using constant properties. It is soil properties that are independent of stress-level and void ratio that is the reason NorSand, and other similar state-parameter based models, are referred to as "good" models. Good models *predict* the effect of void ratio on all aspects of soil behaviour. This prediction is what distinguishes modern state-based models from the plasticity models of the 1980's where properties had to be varied from sample to sample depending on the sample's initial conditions.

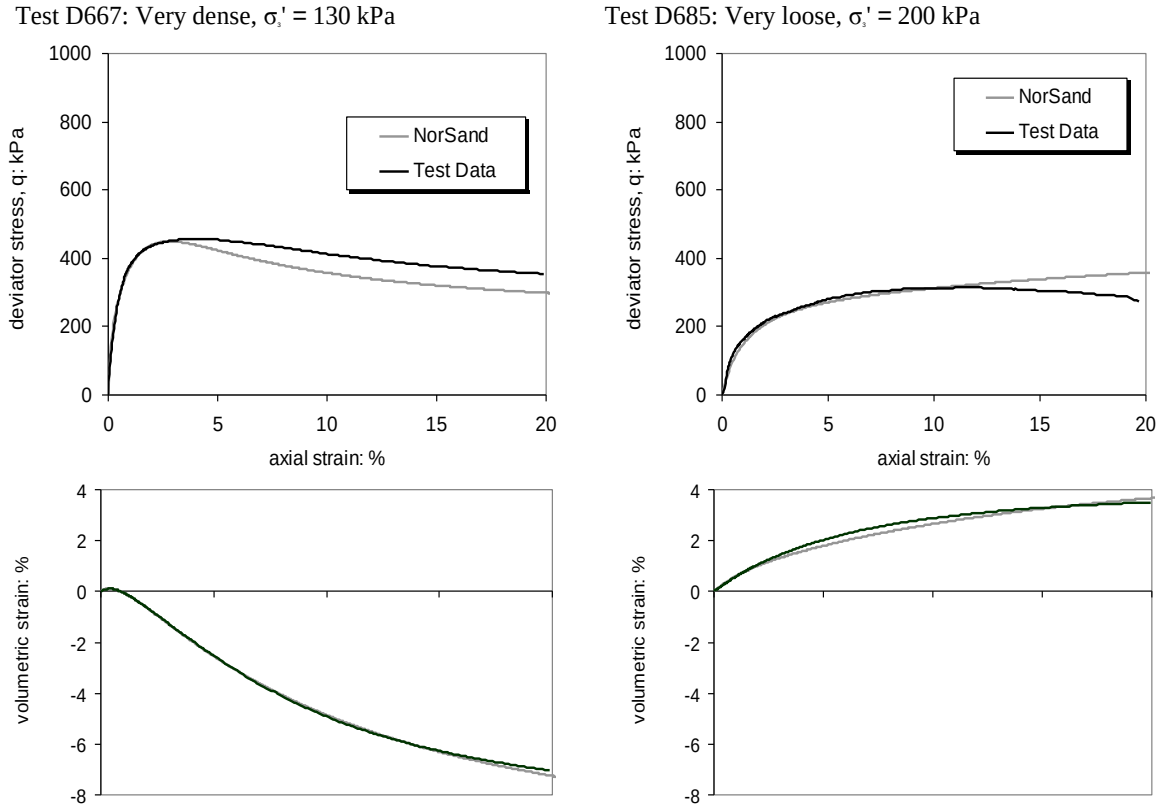

Figure 21. NorSand fit to measured sand behaviour in triaxial compression

Although NorSand involves equations that may appear complicated, it is not difficult for practical engineers to use: NorSand largely uses conventional soil properties of geotechnical engineering. Perhaps the only unfamiliar property is the plastic hardening modulus H, but this can be viewed as similar to the initial plastic shear stiffness in triaxial compression; more usefully, a first approximation is $H \approx 10/\lambda_{10}$ and which illustrates that the slope of the CSL is a plastic compliance exactly as in both Original and Modified Cam Clay. NorSand properties are summarized on Table 1 with an indication of the typical range of values encountered in sands to sandy silts.

Table 1. NorSand Soil Properties with Typical Range for Sands

Property	***Typical Range***	***Remark***
Critical State Locus		
Γ	0.9 –1.4	'Altitude' of CSL, defined at 1 kPa
λ_{10}	0.03 – 0.20	Slope of CSL, defined on base 10 logarithm
Plasticity		
M_{tc}	1.2 – 1.5	Critical friction ratio in triaxial compression
N	0.0 – 0.5	Volumetric coupling coefficient in stress dilatancy
χ_{tc}	2.5 – 4.5	State-dilatancy coefficient in triaxial compression
H	50 – 500	Plastic hardening modulus for loading, often f(ψ)
Elasticity		
I_r	100-800	Dimensionless shear rigidity, G_{max}/p'
ν	0.1 – 0.3	Poisson's ratio, commonly 0.2 adopted

STATIC LIQUEFACTION

This paper started by showing that the widely-held view of static liquefaction being caused by collapse of a metastable particle arrangement was inconsistent with test data when that data was viewed in terms of mobilized stress ratio. We now use NorSand to show the nature and evolution of static liquefaction.

No new and/or changed soil properties are allowed when using NorSand to look at liquefaction. The undrained condition is a boundary condition. In the case of undrained laboratory tests, the drainage valve is shut and that shutting action of shutting the valve cannot change the soil properties. In the case of field situations, an undrained condition arises when the rate at which excess pore pressure is created is quicker than the drainage time.

The basic condition for undrained loading, neglecting the minimal elastic compressibility of soil particles and the pore water, is that

$$\dot{\varepsilon}_v = 0 \quad \Leftrightarrow \quad \dot{\varepsilon}_v^p = -\dot{\varepsilon}_v^e \qquad [11]$$

The implication for the individual volumetric strain components arises from invoking the fundamental strain partition of [1]. Plasticity models capture undrained conditions by calculating plastic strains exactly as for the drained case, and then invoking [11] to obtain the required no volume change condition. The change in mean effective stress (and thus excess pore water pressure) immediately follows by using the elastic bulk modulus *K*:

$$\dot{p} = -\dot{\varepsilon}_v^p \, K \qquad [12]$$

The effective stress change in undrained loading responds only to the shear component of load. An external load increment that increases the total mean stress produces an equal response in the pore water pressure for fully saturated soils (i.e. with $B = 1$). Partial saturation effects or finite pore water compressibility can be added in easily enough, using $B < 1$ and computed from compatibility of volumetric compressive strain (although doing so provides no further insight and is not discussed further).

Equation [12] shows the importance of elasticity to undrained behaviour. This presents a problem because elastic stiffness is sensitive to soil "fabric" (the arrangement of soil particle contacts). Practically, the elastic shear modulus (G_{max} as it is commonly known) is measured geophysically using shear wave propagation velocity (measured by bender elements in the laboratory, seismic CPT in the field) and that should be routine practice. However, *K* is far more difficult to measure as the pore water dominates

compression wave velocity. Thus, the approach is to measure *G* and then relate *K* to measured *G* through Poisson's ratio (ν) and relying on Poisson's ratio apparently lying in the limited band $0.15 < \nu < 0.25$ for soils.

Figure 22 compares NorSand with the three undrained liquefaction tests representing the spectrum from highly contractive to lightly dilatant. In fitting the tests, *H* and I_r have been varied around the mean trends to obtain the best fit to the stress strain data, with the parameters used being shown for each simulation. All other soil properties are the same as the dense calibration. These simulations can readily be repeated using the downloadable *NorSand.xls.* It is emphasized that the good fits are obtained using parameters calibrated from dense drained triaxial tests and explicitly without a collapse surface (which does not exist in NorSand).

Test L601 was a lightly contractive sample with an initial state $\psi_0 = +0.025$. The peak strength and onset of liquefaction is nicely predicted. The subsequent strength drop with increasing strain is less dramatic in NorSand than the experiment, but this may be a rate or inertial effect as the experiment was load controlled. A little overconsolidation ($R = 1.15$) was introduced to replicate soil structure effects that affect the initial shape of the stress path, with a good fit to the stress path overall.

Perhaps the most dramatic aspect of the undrained response of sand is the static liquefaction of very loose samples. The loosest sample tested in undrained compression was sample C609 with $\psi_0 = +0.068$. Using unchanged material properties, a good fit to the measured behaviour is computed including the characteristic extreme post peak strength drop of very loose samples as illustrated on Figure 22. Less dramatic behaviour is the undrained response of lightly dilatant sand and Figure 22 shows C634 with $\psi_0 = -0.08$.

Having demonstrated that NorSand predicts the measured response of sand in undrained triaxial shear, including what are conventionally termed liquefaction tests, it is now possible to examine the nature of static liquefaction by looking into the details of NorSand. When a loose sample is loaded undrained, contractive volumetric strain occurs but these sequences themselves are not the cause of liquefaction. In liquefaction, volumetric contraction has the effect of reducing the mean effective stress by much more than the shear strength gain induced by these same strains hardening the yield surface; recall that NorSand has a hardening limit, and in the case of soil with $\psi > 0$ this hardening limit forces the yield surface to contract (soften) in moving to the critical state. Further, the role of elastic and plastic strain in the generation of excess pore pressure implies that the ratio of plastic hardening to elastic shear modulus (λ/κ in Cam Clay or I_r/H in NorSand) will be important soil strength and other aspects of undrained soil behaviour – most readily seen by running a few simulations using *NorSand.xls*.

So far this discussion of liquefaction has been focused on laboratory situations. Now consider a field situation, say a slope being loaded and/or steepened and where the situation is clearly drained to start. Potentially, brittle collapse can arise with any strain softening stress-strain behaviour. For saturated soil, water must be displaced out of the pore space as loose sand is sheared and the stress path is controlled by the rate at which shear strain is applied versus the time to dissipate the excess pore pressure. Now we will consider the undrained strength that develops from differing (drained) K_0 situations, a set of scenarios that illustrate how the mobilized shear stress at failure might change depending on how much of the loading path is drained and how much is undrained.

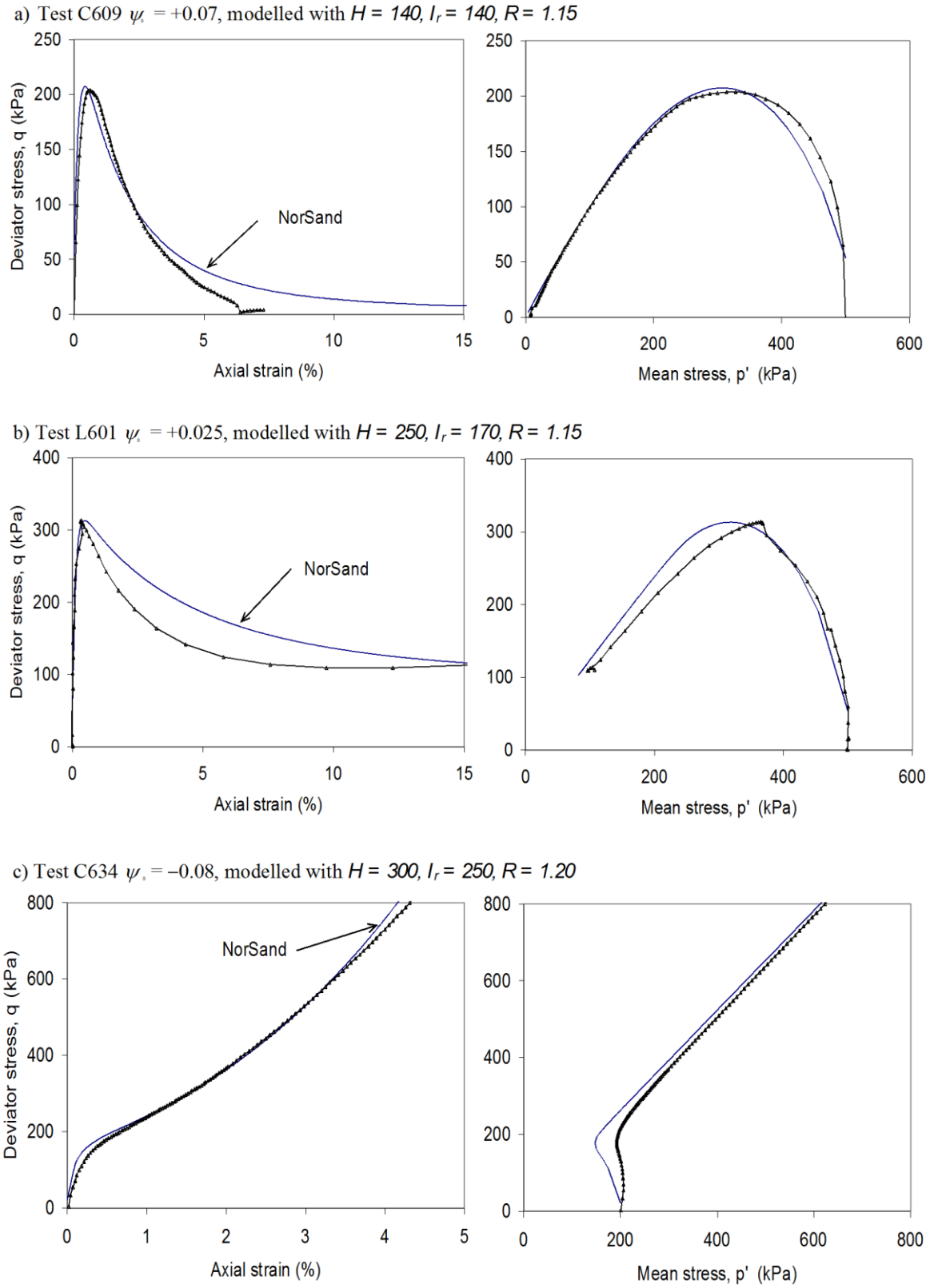

Figure 22. NorSand predictions of undrained behaviour of Erksak sand using soil properties determined from drained triaxial compression of dense samples

Because interest in static liquefactions is in the context of loose soils, some example simulations were carried out using the Erksak 330/0.7 calibration of *NorSand* and for an initial state parameter of ψ_0 = +0.05. This is actually rather loose, being midway between the extreme liquefaction shown on Figure 22a and the less brittle behaviour of Figure 22b. Partly, the rather extreme behaviour derives because Erksak is a relatively stiff sand, so things tend to happen quickly compared to more silty materials. A common mean stress level of 200 kPa was chosen for the simulations, which is a not unusual value for a field slope or fill. The simulations started from a range of K_0 situations, these being equivalent to the end of a drained loading path before onset or transition into undrained behaviour.

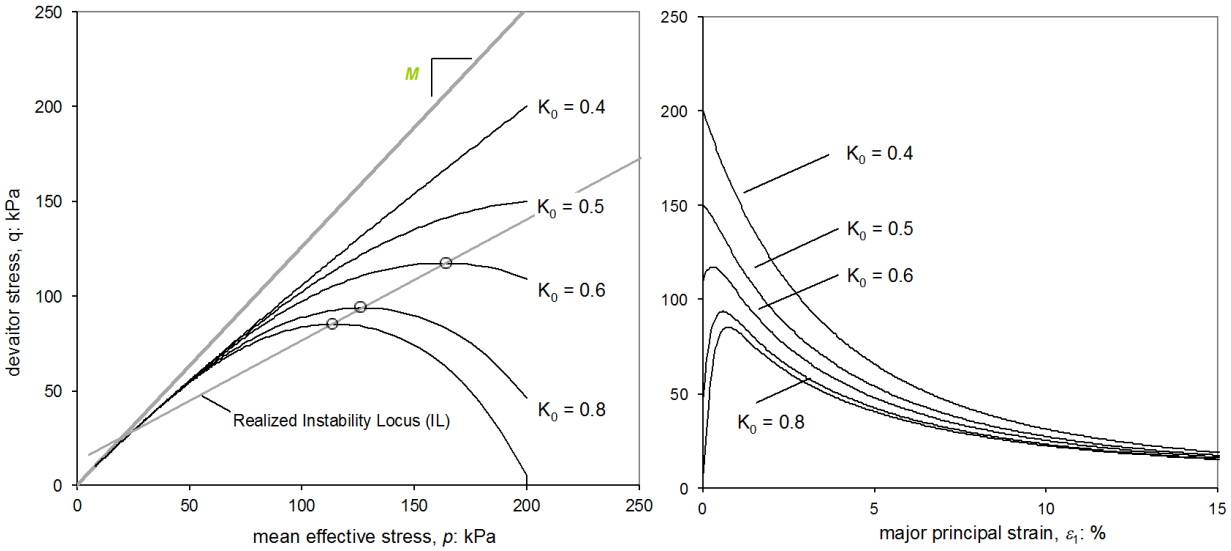

Figure 23. Simulation of static liquefaction from various geostatic stress states

The results of the simulations are shown on Figure 23. There is an increase in undrained strength as K_0 decreases (increased initial shear stress), a consequence that a smaller part of the strain path is in the weaker undrained mode. But this process only goes so far. In the case of the simulations shown on Figure 23, once $K_0 < \approx 0.55$, then strength immediately and rapidly falls after the switch to the undrained mode – this behaviour is most clearly seen on the stress strain curves. This transition to an immediate strength drop arises at far below the drained strength. Why did this not arise in the loose drained laboratory tests we discussed earlier? Because those laboratory tests were carried out using displacement control to demonstrate that there was no metastable collapse in the arrangement of sand particles. What we are exploring here using *NorSand* is the effect of drainage conditions when simulating load control. And what is apparent is that despite NorSand having no concept of an instability locus (IL) in its formulation, the locus through peak strengths of the semi-stable simulations (circled on the respective stress paths) is a straight line and predicts the limiting K_0 at which semi-stable behaviour is possible.

A further set of simulations were carried out to extend the range for this instability locus (IL) and ascertain whether changing stress level (while keeping ψ_0 constant) produced the same IL. The results are shown on Figure 24. A constant state but greater stress level does not fall on the same instability locus (IL). But setting a slightly less dilatant state, equivalent to holding void ratio constant, does sensibly fit the same IL.

Let us now reiterate the important point: the IL is a soil behaviour, not a property of the soil. The hardening limit, equation [8] and which involves the soil property χ and the current state parameter, combines with the plastic modulus H and elastic bulk modulus K, to establish the IL. Whether collapse develops then depends on the possible transfer of load through stress redistribution.

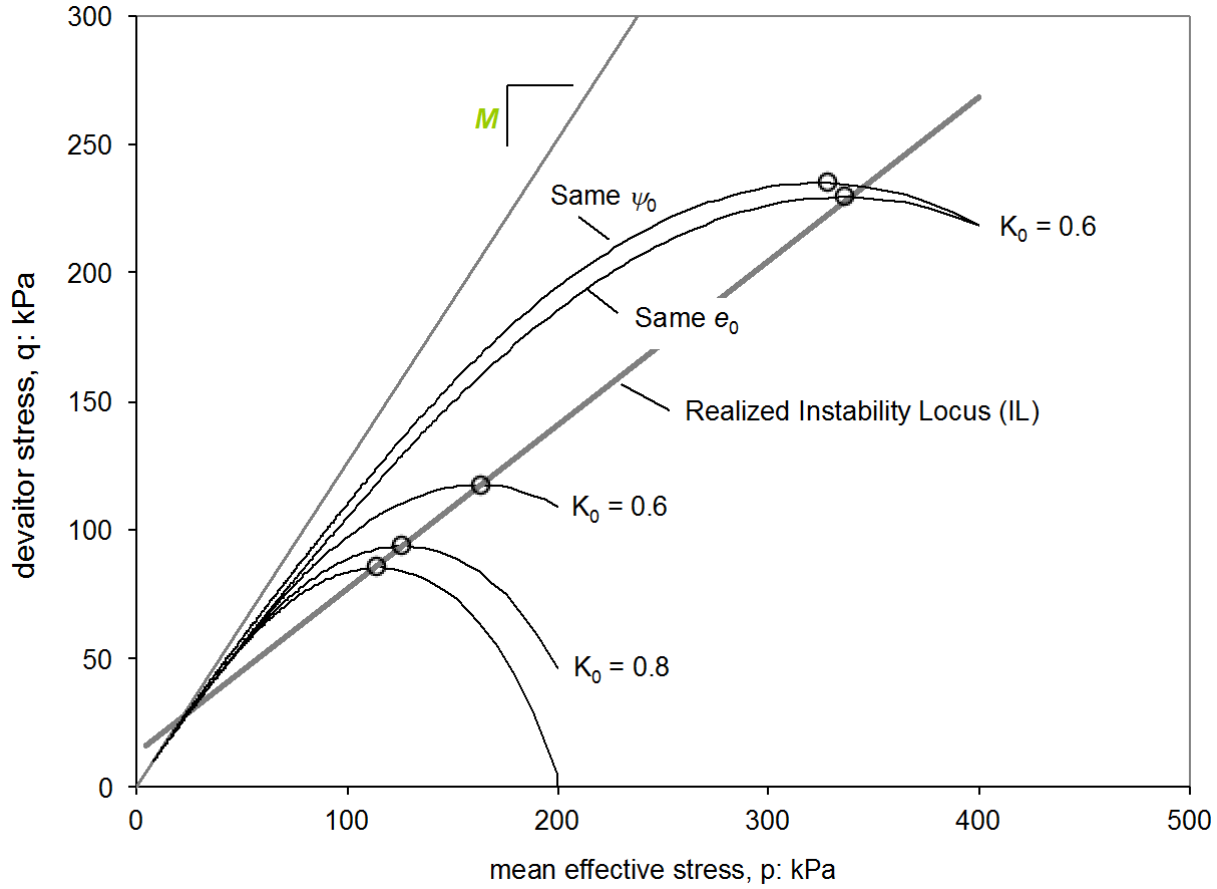

Figure 24. Effect of stress level on static liquefaction

We can take this a step further and use NorSand to predict the stress ratio at instability (η_L) as a function of changes in the elastic and plastic modulus. Figure 25 shows the results when this is done, for a particular set of soil parameters and one initial state (ψ_o = 0.065). For this choice of soil properties and state the instability stress ratio can vary easily from η_L = 0.75 to η_L = 1.0 for the same value of critical friction ratio M_{tc}.

The peak undrained shear strength and pore pressure generation (triggering of liquefaction) cannot be represented by an effective stress friction ratio or instability line as a soil property.

Practically, these results mean engineering to resist liquefaction requires consideration of soil stiffness, both elastic and plastic, as well as soil state. In itself, this has been known for many years and is a consequence of any good constitutive model. But, present liquefaction practice focuses on *fines content* as an indicator of stiffness neglecting (or more truthfully, dismissing without justification) a large body of test data that shows fines content to be a very poor predictor of soil stiffness. However, this deficiency in present practice is becoming more recognized with, for example, the recent 5th International Earthquake Engineering Conference in 2011 having perhaps a quarter of the contributions calling for routine measurement of G_{max}. A routine practice demands no more than about every four to five CPT's at a site being carried out as seismic CPT with logging of shear wave velocity profiles.

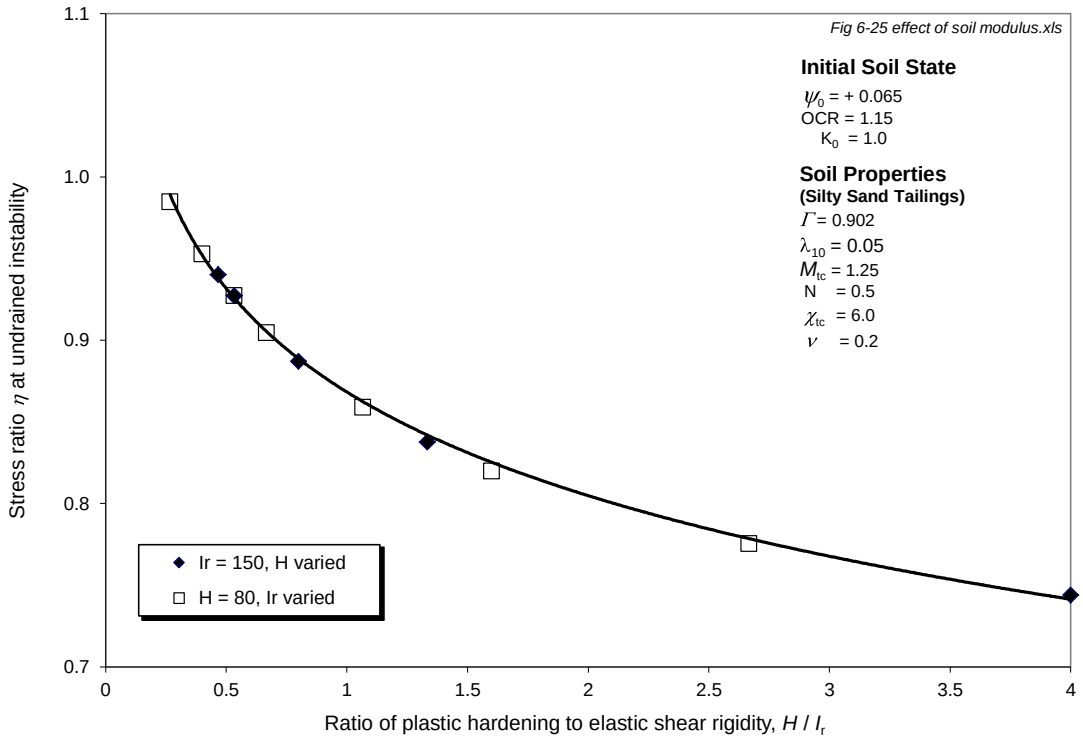

Figure 25. Computed effect of soil stiffness on instability locus for liquefaction

SILT BEHAVIOUR

So far this paper has presented the thread of theoretical developments that resulted in critical state soil mechanics, and then shown how insight from the large-scale behaviour of sands provided a full generalization of the framework with two 'state' measures being needed: OCR and ψ. What has been somewhat obscured in this attention to 'the math' is the nature of the soils being represented.

The early contributions of Reynolds and Casagrande were about sands. However, although the framework of Drucker et al. looked to both sands (with the critical state) and clays (closed yield surface intersecting the NCL), the developments from that framework to produce Cam Clay were based on test data on clays. Then, the generalization of Cam Clay into NorSand returned to sand behaviour. This leads to a reasonable questioning of whether the various models are specific to particular soil types, perhaps as indicated by the model names (i.e. only use Cam Clay for clays etc), and where silts might lie in this spectrum of sand to clay.

All critical state models are theoretical constructs tracing back to the Second Law of Thermodynamics and with some simple idealizations about particulate behaviour. The model names derive from the academic limitation that if the model is cited as 'Bloggs et al.', nobody but Bloggs et al. will use the model – to make a framework of ideas widely accepted requires that the ideas be depersonalized. Schofield & Wroth were aware of this issue and chose to give a somewhat neutral name to their set of ideas, which then established the protocol that developers of critical state type models would combine the name of the developer's adjacent body of water with a soil type. Hence Cam Clay after River Cam, Superior Sand after Lake Superior, Severn-Trent Sand after the River Severn etc. Regardless of name, all these models address the constitutive behaviour of particulate materials with no bonds between the particles (these do not even have to be soils); the actual particle size (which determines whether a soil is viewed as sand, silt, or clay) is irrelevant to the physics and the mathematics, although the numerical values of the properties will vary.

Given this background to model names, it is reasonable to view silts as a "test" of model generality since data from silts has not been used in any of the developments. Of course, a difficulty here is that silts are rather difficult materials to test in the laboratory. Reconstituted silt samples are much more difficult to produce than reconstituted sands directly in a test, but equally the extrusion and trimming of 'undisturbed' silt samples causes the tested void ratio to be denser, sometimes much denser, than the original sample. However, the minerals "boom" of the past decade or so has seen the engineering of some very large dams to retain, or even built on, silts. Strength testing of silts is now routine for many engineering companies, although the corresponding need to deal with the consequence of sample disturbance remains poorly understood – and is an issue we will return to later in this paper.

An example of data of a pure silt tailings (100% finer than #200 sieve) from a large copper mine is shown on Figure 26. This sample, after consolidation to the test pressure, was loose of the critical state with ψ_0= 0.078. It was a compressible soil, unsurprisingly for a silt – with λ_{10} = 0.233. As illustrated on Figure 26, NorSand readily matches the measured behaviour using the measured CSL – the effect of changing gradation from "sand" to "silt" is fully reflected in the changed λ_{10}. It is not soil gradation itself that matters, but rather how soil gradation alters the mechanical properties λ_{10} (and thus also H) and G_{max} that control the soil response to loading.

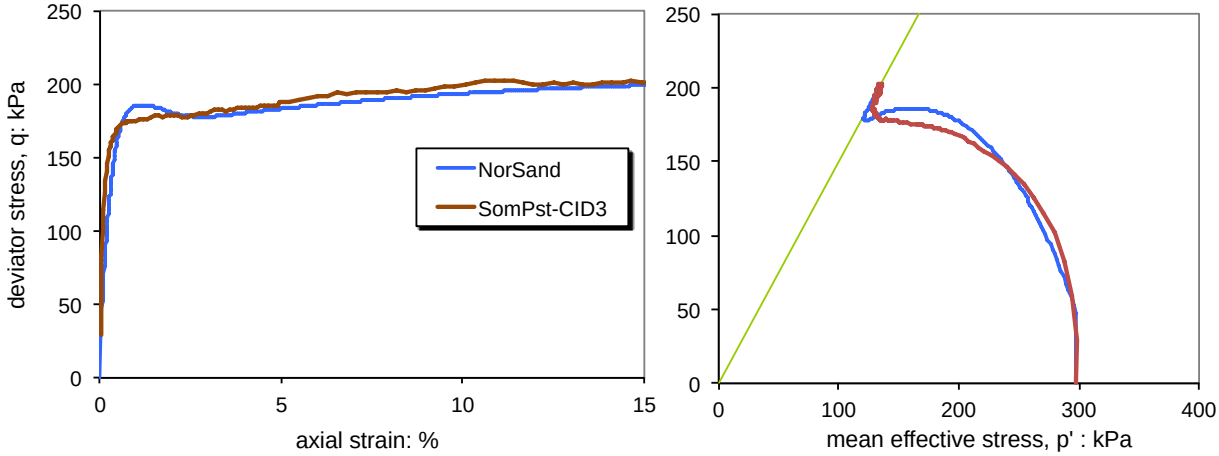

Figure 26. Undrained triaxial compression of loose silt

More generally, the fit of NorSand to the silt data shown on Figure 26 substantiates that critical state mechanics applies to silts. CSL exist for silts and are readily measured (see Figure 5). The state measures of ψ and OCR apply. And using the same mechanical properties as exist for sands and clays produces stress-strain curves that match data. The only 'issue', if it can be called that, with silts is that they tend to be more compressible than sands but with a stronger effect of void ratio on their behaviour than arises with clays.

MEASURING THE STATE PARAMETER INSITU

Overview

Simplifying somewhat, the work presented so far can be summarized as:

"*Soil behaviour = Properties × State*"

Soil properties can be measured in the laboratory because they are independent of void ratio, but these properties are not enough without knowing the insitu soil state. Practically, because of the difficulty in sampling sands in anything like an undisturbed condition, measuring sand state depends largely on penetration tests. Silts offer the possibility of directly measuring void ratio (for saturated samples) using thin-wall hydraulically pushed samples but this tends to be both expensive and slow; engineering of silts

therefore also tends to rely on penetration tests but with the now added complication that penetration will generally be undrained. Let us now consider penetration tests to determine insitu soil state in both sands and silts.

Soil properties can be measured in the laboratory because they are independent of void ratio, but these properties are not enough without knowing the insitu soil state. Practically, because of the difficulty in sampling sands in anything like an undisturbed condition, measuring sand state depends largely on penetration tests. Silts offer the possibility of directly measuring void ratio (for saturated samples) using thin-wall hydraulically pushed samples but this tends to be both expensive and slow; engineering of silts therefore also tends to rely on penetration tests but with the now added complication that penetration will generally be undrained. Let us now consider penetration tests to determine insitu soil state in both sands and silts.

Penetration tests are simple and inexpensive, attributes that allow large numbers of tests to characterize the variability of ground properties in the strata of interest. Today, penetration tests mean the use of electronic piezocone CPT – the equipment is accurate, reliable, repeatable, and records data digitally. Although original interest in the CPT derived from the geologic perspective of stratigraphic identification using a continuous record, it is the repeatability and accuracy of the test that is of most interest here. The determination of penetration resistance to an accuracy of typically better than 2% is certainly precise enough for soil testing and provides the basis for estimating the state parameter insitu.

CPT resistance is very dependent on the stress level, all other factors being equal. The first step in evaluating CPT data is to remove the effect of stress level, which in a framework of applied mechanics means changing to dimensionless CPT parameters. A dimensionless approach allows scaling through the laws of mechanics and avoids adjustments or "corrections." Thus, tip resistance q_t is normalized by the mean effective stress in the ground before the penetration test (p'_0) to give the dimensionless penetration resistance $Q_p = q_t/p'_0$. For the other CPT data of sleeve friction and pore pressure the corresponding dimensionless parameters are F and B_q respectively. All these dimensionless parameters are common in the CPT industry, and they form the basis for determining the insitu state parameter for all soil types.

Measuring ψ in sands

Despite the simplicity and accuracy of the CPT, so far it has not proved possible to develop full theoretical solutions that could form the basis for determining soil state. The CPT is a difficult problem: penetration is essentially a continuous flow situation with a high degree of confinement, and the soil close to the CPT goes from at rest conditions to the critical state as it is sheared by the CPT. Reasonable understanding can only emerge from large strain analysis with a good soil model. Such good soil models are not analytically tractable. Thus, most interpretation of the CPT in sand is based on large calibration chamber (CC) testing in which CPT response is measured under controlled conditions to develop a mapping between response and some combination of sand density and stress. But, there is no unique mapping applicable to all sands and only a few sands have been tested. The approach that has developed is to use cavity expansion as an analogue of the CPT resistance, calibrate that analogue to existing CC data, and then use the calibrated analogue to develop the general framework.

Most calibration chamber (CC) work has been carried out by universities using standard laboratory clean sands. When the state parameter framework was developed, samples of these various sands were obtained and the CSL of each determined. This then allowed immediate re-processing of existing CC data into state parameter form (Been et al, 1986, 1987). This capturing of existing data was then supplemented by construction of a new, large CC chamber to test the actual sand being used in the hydraulic fill construction discussed earlier in this paper. Figure 27 shows this calibration chamber – a typical sample involved about 2000 kg of sand placed uniformly and at constant and varied density (from loose to dense).

The results of calibration chamber tests involve judgment: the measured q_t is rarely constant and there is also some variability on the soil void ratio within the chamber. So, even though the CC is viewed as the "gold standard" for evaluation of CPT data in sands, there is a noticeable scatter in the results. Figure 28

shows the eventual form of data from a CC test program with judged characteristic penetration resistance plotted against initial mean effective stress and with the characteristic state parameter for each data point indicated. The data contours as radial lines of constant state parameter. All sands show similar behaviour.

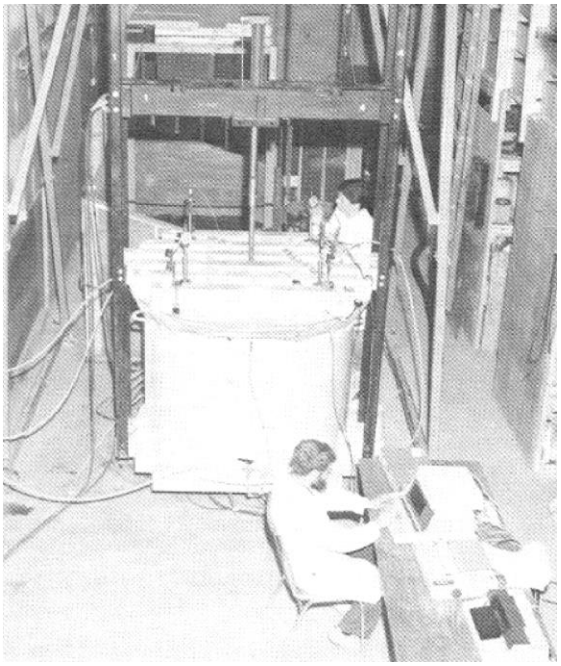

Figure 27. Example of large CPT calibration chamber

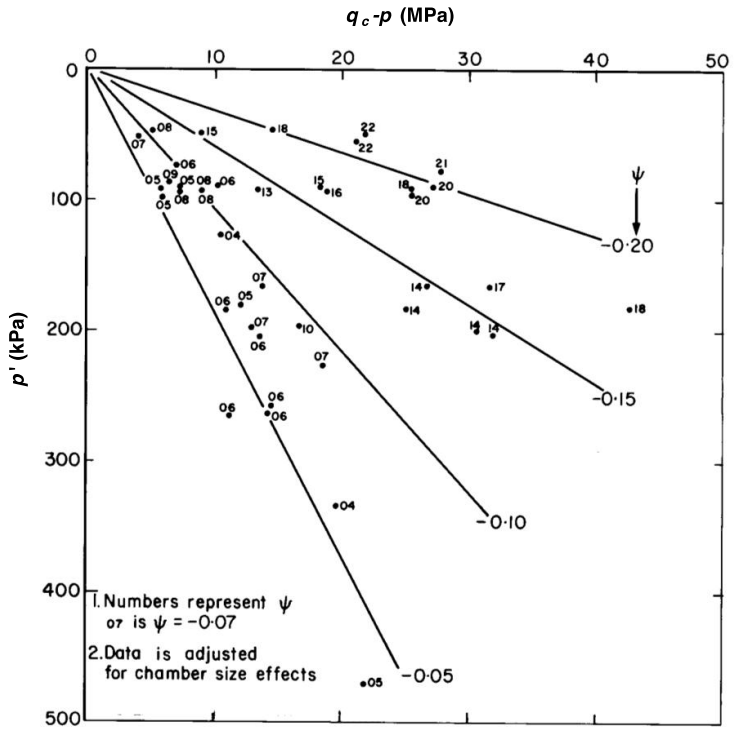

Figure 28. Example of processed data from calibration chamber testing

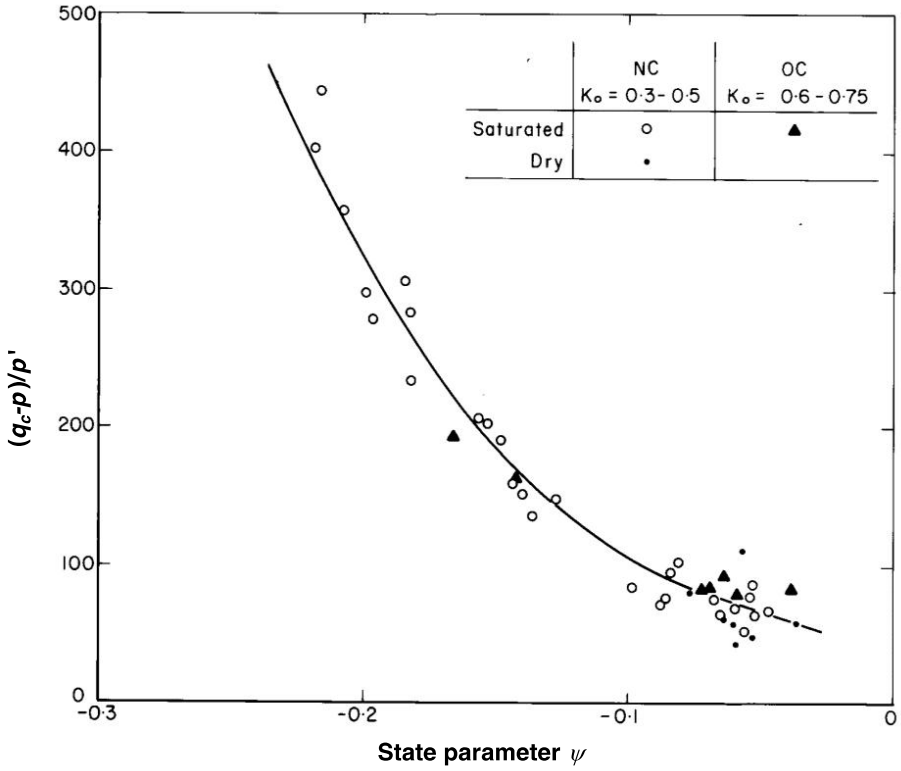

Figure 29. Normalized trend in calibration chamber data – Monterey Sand

Radial contour lines correspond to constant values of Q_p. The data shown on Figure 28 therefore reduces to a simple plot of Q_p versus ψ, shown on Figure 29. The trend line shown on Figure 26 has the delightfully simple form:

$$Q_p = k \exp(- m \psi) \qquad [13]$$

Equation [13] has proven universal for all sands calibrated to date, although the coefficients k and m differ from one sand to another. This differing response of differing sands to the CPT is not particular to the state parameter approach; the same issue arises if the CC data is viewed in terms of void ratio or relative density. Soil properties as well as sand state affect the response of the sand to the CPT.

The difference in the CPT calibration between quartz sands and sands containing softer minerals can be quite large – under conditions involved with liquefaction assessment determining appropriate k and m values for the site-specific soil is a crucial task. The same task also exists if the assessment is done in terms of relative density, so this is not an impediment to adopting the state parameter but rather the reverse: only the state parameter approach offers a proper basis for assessing which relationship applies to a particular sand, which is now discussed.

Quantification of how soil properties affect the CPT relies on the cavity expansion analogue. Cavity expansion is an idealized situation where soil is displaced symmetrically away from a point; the symmetry can be cylindrical or spherical, with understanding of the CPT adopting spherical symmetry. When a cavity is expanded, at some finite displacement the pressure to continue that expansion becomes constant; the analogue is that this limiting cavity pressure corresponds to the tip resistance of the CPT. The attraction of the cavity analogue is that a complex 3D problem is changed to a symmetrical situation in terms of radial displacement alone – straightforward for numerical analysis with finite displacement method and using sophisticated constitutive models.

There is a long history of cavity expansion methods in geomechanics, for example they are part of all pile capacity formulae. A particularly useful semi-closed form of cavity expansion analysis was presented by Carter et al (1986) using constant friction and dilation angles (which do not need to be equal); this idealization being the simplest reasonable idealization of frictional soil behaviour. If the friction and dilation angles are linked using stress-dilatancy theory, and dilatancy is given in terms of the state parameter using [6], the form of [13] is recovered together with the requirement that the relationship must include the parameter group G_{max}/p'_0 as a scaling factor on k.

Cavity expansion analysis was undertaken using NorSand to explore how soil properties and stress level affected the CPT. The analysis (Shuttle & Jefferies, 1998) used a moving-mesh finite element approach and convected work to represent the needed finite displacement aspect. The calibration factor between cavity expansion and the true CPT was found for Ticino sand with Figure 30 showing the basic results. The scatter in the numerical cavity expansion trend is caused by the range in initial conditions with an 'effect' from initial confining stress that causes variable G_{max}/p_0 in the plotted results. The scatter in the actual CC data partly includes that effect too, but also has considerable experimental scatter – these 'gold standard' calibrations are not as repeatable as many users imagine and it is important to use average trends to remove these experimental factors (recall, a calibration involves near 2000 kg of sand that has to be placed to a precise void ratio…). Thus, the calibration factor C_{cpt} is simply the ratio of these two trend lines: calibration $C_{cpt}= Q_{cc} / Q_{sph}$.

A further consideration was to show that the calibration factor C_{cpt} was not affected by soil properties, confining stress etc. as that is a necessary condition to allow reliance on cavity expansion methods to determine the k and m values used in assessing site data. The assessment used Hilton Mines sand, by far the furthest 'outlier' in published chamber test data. It was found that C_{cpt} was unchanged within the precision of the available data (Shuttle & Jefferies, 1998).

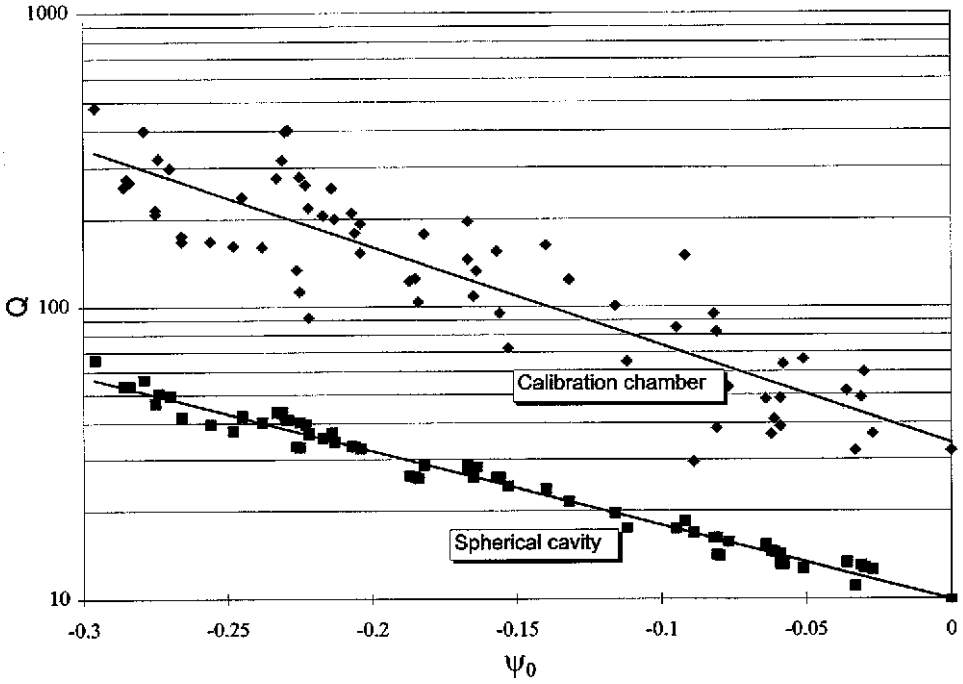

Figure 30. Calibration chamber compared to cavity expansion for Ticino sand

A limitation of numerical methods is that they are numerical – there is no simple equation for practical engineers to use. Two approaches have been adopted to deal with this situation. First, the finite element cavity expansion solution has been developed into a stand-alone executable ("the widget") that takes the NorSand soil properties as input and which generates results for importing into Excel for engineers to best-fit trend lines and develop their best-estimate k and m values for those soil properties. Second,

numerous parametric simulations were carried out to develop influence factors for the soil properties on k and m. The first approach is more accurate but also more time consuming; the widget will shortly be in the public domain but is presently only available 'on request'. The second method is less accurate, but readily implemented as a user-defined function in Excel and is very practical; it is in the public domain with all the factors being provided in Shuttle & Jefferies (1998).

Measuring ψ in silts

There is very little calibration chamber for silts and with uncertainty over chamber size effects for what slit calibration data that does exist. However, cavity expansion analysis applies to all soils. As NorSand has been validated for capturing the constitutive behaviour of sands, silty sands, silts, and well-graded (till-like) soils – and with substantial detail – so that cavity expansion of NorSand can be applied across a wide range of soils provided that care is taken with the transition from drained penetration (sands) to undrained penetration (sandy silts and finer gradations).

The NorSand cavity expansion approach was extended to undrained behaviour by Shuttle & Cunning (2007), with an effective stress version of equation [13] emerging as:

$$Q_p(1-B_q)+1=\bar{k}\exp\left(-\bar{m}\,\psi\right) \qquad [14]$$

…where the parameters $\bar{k}$ and $\bar{m}$ use the "bar" notation to distinguish them from k and m for drained CPT penetration. Of course, for drained penetration with B_q=0 the approach becomes identical with [14] essentially reverting to [13] if the "+1" term is neglected (typical Q_p > 50 for what would be regarded as loose sands, so this neglect is reasonable). Equation [14] has been used for some time, the idea originating with Been et al. (1988) from considerations of the similarity between ψ and OCR and using this to link trends seen in CPT response in sands and clays; the importance of the Shuttle & Cunning result was in it that provides a rigorous basis to what was previously a pragmatic deduction.

DEALING WITH NATURAL SOILS

Including Soil Properties

Both calibration chamber tests and finite element cavity expansion simulations show that the mapping between Q_p and ψ (or D_r) depends on the soil properties. Further, this is not just a minor detail for liquefaction assessment: put in relative density terms, for a particular q_t value from the CPT one calibration could indicate 60% relative density (which would have generally adequate liquefaction resistance) while an alternative calibration could indicate 40 % relative density (implying likely ground improvement). The engineering decision on needed actions can depend as much on the calibration as on the measure penetration resistance.

Soils insitu differ considerably from the sands used for CC studies in three respects: 1) insitu sands will commonly have at least a few percent silt, and often significantly more; ii) insitu sands may have sufficient fines that penetration is no longer drained; and, iii) insitu soils show considerable variability in gradation from place to place even within a "uniform" stratum. On a wider scale, moving from sands to clays, the critical friction ratio M decreases, the compressibility λ increases, and the plastic hardening H decreases. All these changes in soil properties affect the penetration resistance. A key question then arises: in assessing CPT data, how can the effects of soil type be differentiated from the effects of soil state?

In the case of uniform soils, it is reasonable to recover representative samples to test and so determine the soil properties. This gives a basis for selecting a Q-ψ relationship, but does not respond to the issue of soil type variability within the stratum. Nor does it respond to the issue that many projects will not support extensive (or even any…) laboratory testing. Both these concerns were addressed using the idea that soil properties can be estimated from soil type and that soil type can be estimated directly from the CPT using the measured Q, F, B_q data. Certainly, this is a less precise approach than measuring soil properties, but very quick 'to do', working with the CPT data alone. The approach is sometimes referred to as a 'screening level' assessment to reflect the increased uncertainty in the results compared to

processing the data using a site-specific calibration. The screening level assessment applies across all soil types.

Screening Level Assessment

The starting point for understanding screening of a level assessment is the observation that CPT behaviour from sands through to clays can be fitted by extending equation [14] to account for drained through to undrained conditions. Using this equation, Been et al. (1988) linked trends in the penetration resistance of sands and clays, making the further assumption that soil compressibility and plastic hardening were functions of λ_{10} (inferred on the basis of Cam Clay). Taking the various clay and sand calibrations produced the relationships:

$$\bar{k} / M = 3 + \frac{0.85}{\lambda_{10}} \qquad [15a]$$

$$\overline{m} = 11.9 - 13.3\lambda_{10} \qquad [15b]$$

The next step is to estimate λ_{10} from the CPT data. Plewes et al. (1992) suggested that there was a linear scaling between the soil property λ_{10} and the dimensionless friction ratio *F* measured by the CPT itself. This suggestion has stood the test of time and has been improved with additional data resulting in Figure 31.

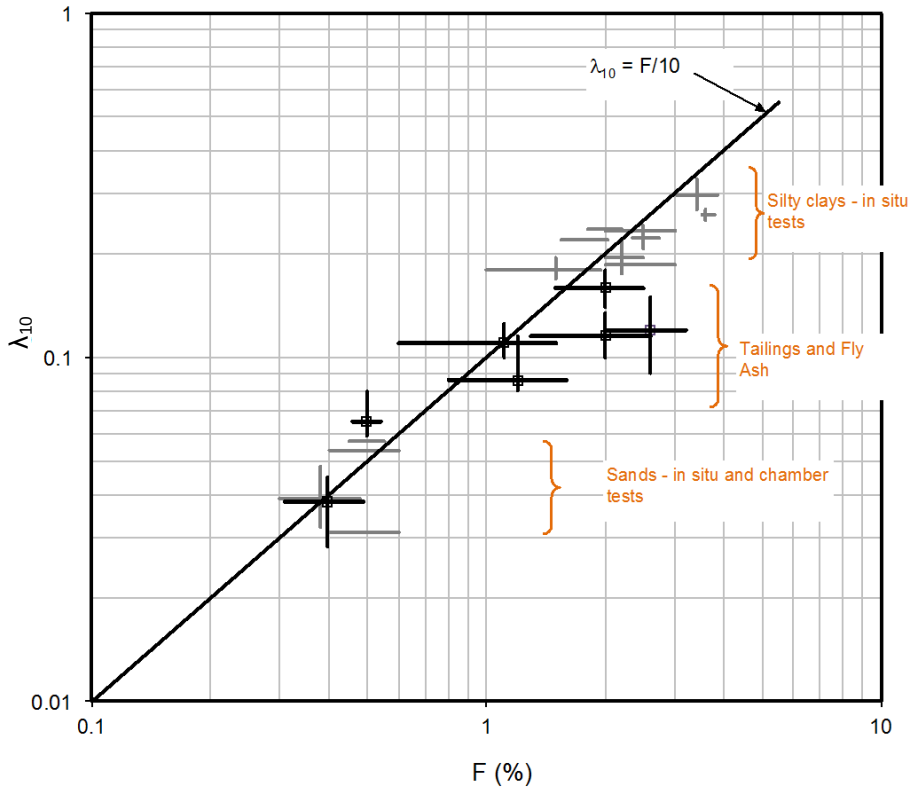

Figure 31. Correlation between slope of CSL and friction ratio in CPT (Reid, 2014)

The trendline through the data on Figure 31 is:

$$\lambda_{10} = F / 10 \quad \text{(with } F \text{ in \%)} \qquad [16]$$

The screening level assessment can be considered as a form of soil behaviour type classification that also includes ψ. Figure 32 illustrates the approach by showing the results of equations [14], [15a,b] and [16] on a single chart as green contour lines that is a broadly orthogonal to the soil behaviour type contours. This form of relationship was first proposed by Shuttle and Cunning (2008) and proves to be an extremely useful "first look" at CPT data in practice; it is also trivial to implement in CPT processing software.

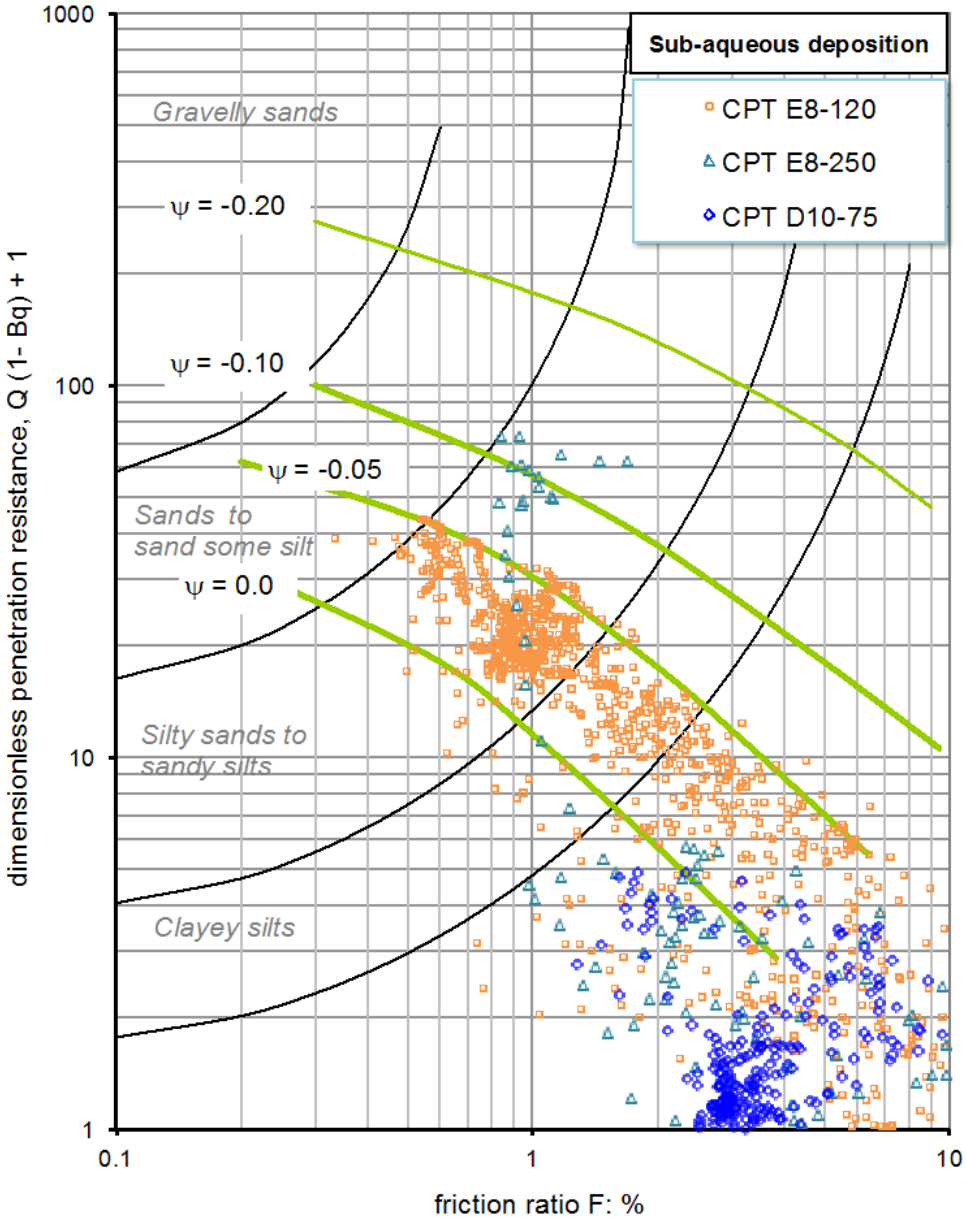

Figure 32. Screening level chart for assessing CPT data in terms of soil behaviour type and insitu state parameter

The idea of a smooth trend in normalized CPT resistance across the full range of soil types (that is, the green lines on Figure 32) was a hypothesis when proposed by Been et al (1988). The subsequent work of Shuttle & Cunning (2007) looked at two calibrations in sand and one in very loose silt to define their criterion for static liquefaction vulnerability. It is reasonable to question these smooth trend lines. Some recent investigations in mine tailings allow some resolution of the issue.

The mine waste (tailings) from crushing rock to recover the metals produces large volumes of sands and silts. Most mines transport these soils as hydraulic slurry and discharge them into 'tailings management areas' that are confined by valley sides and perimeter dams; the tailings largely accumulate under water apart from a near spigot beach. As the volume of tailing accumulates the retaining dams are raised. These perimeter dams are now engineered structures with dam raisings often being accompanied by CPT investigations of the tailings upstream of the dam.

The results of three soundings in sub-aqueous tailings are shown on Figure 32, with each point corresponding to approximately 50 mm depth intervals of the measured data. These sounding typically comprise an overall thickness of 10 m to 15 m of sub-aqueous tailings. In the case of the tailings at the location of sounding E8-120, segregation of the tailings into silty sand is evident, with interbeds of more silty tailings; presumed caused by meandering of the deposition stream over the underwater slope as the tailings sedimented.

Regardless of segregation, the tailings develop an approximately constant state parameter in their "normally consolidated" condition at $\psi \sim -0.03$ and following the Been et al (1988) hypothesized trend from silty sand through to pure silts. This behaviour has been encountered at other tailings sites and is thought to be a "geological principle": particular depositional conditions produce a particular state regardless of the differing soil gradations involved.

Sounding D10-75 is furthest from the historical spigot locations and shows only the silt ("slimes") component of the original tailings stream. These silts are looser than their critical state, and looser than weak natural clays that would be characterized as "normally consolidated".

Dealing with Site Variability

The Plewes Method uses average trends in soil properties, and as can be appreciated from the data plotted on Figure 31, the inferred compressibility is within an uncertainty of a factor of two. But, this idea of linking soil properties to the soil behaviour type inferred from the CPT data itself is the only practical possibility for assessing the consequence of geological variability within a stratum.

The limitation of the Plewes Method is also easily overcome. Obtaining and testing soil samples from a known location adjacent to a CPT sounding can be used to obtain a site-specific calibration of the method. Depending on project importance and scale, a calibration for three differing locations can generate an improved site-specific version of Figure 31 together with site-specific versions of equation [15a,b]. Such site-specific calibration of the CPT, and reliance on the CPT to sense variation in soil behaviour type across a site, is certainly "best practice". But, it is also the only realistic option that can be used to assess the consequence of soil variability for a project; it is not too onerous in practice because of the low costs of CPT soundings.

An alternative to the CPT for silts

Undisturbed samples can be recovered using hydraulic push of 'sharp' thin-wall sampling tubes (commonly 75mm diameter). The void ratio can be determined from water content on the cuttings from the sampling tube prior to sealing it for shipping to the laboratory – commonly, the cutting will be captured into small plastic bags and their water content measured on site. Most tailings are located below the water table so saturation can be relied on and the void ratio calculated from the specific gravity of the soil particles combined with the measured water content. An example of data from this method is shown on Figure 33, together with the CSL determined from laboratory triaxial tests. The insitu void ratios are looser than the CSL as would be expected from hydraulic deposition, which provides normally consolidated conditions.

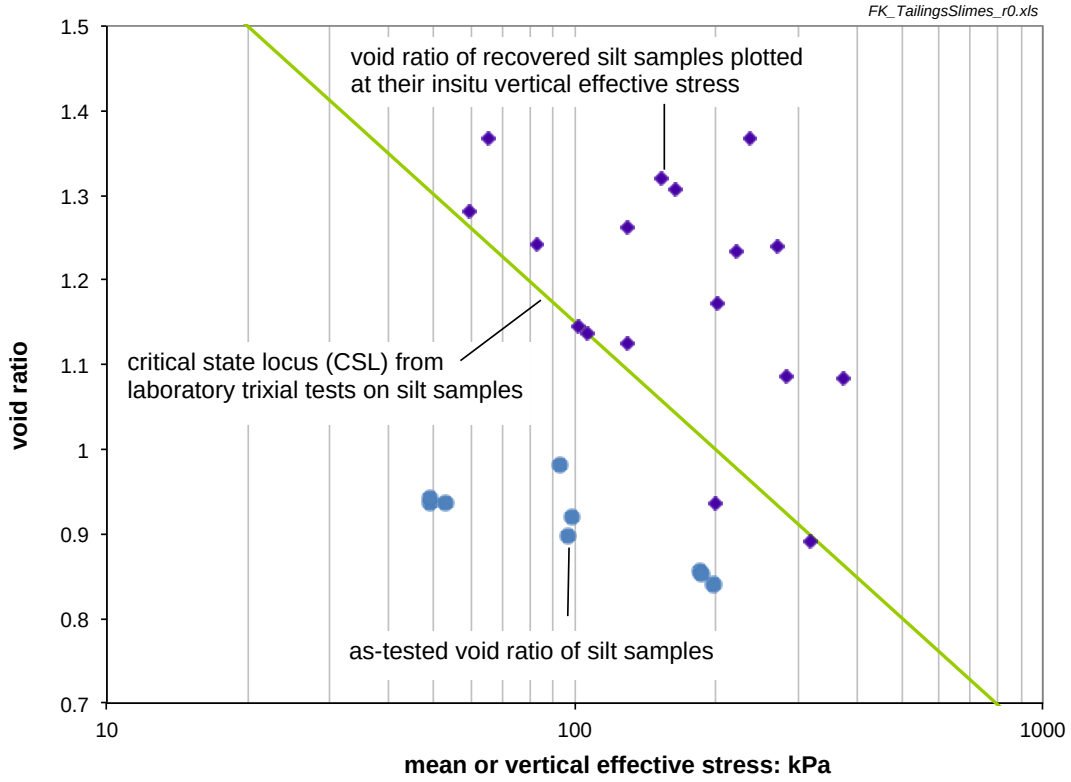

Figure 33. Insitu void ratio of silt tailings from undisturbed sampling

Despite the apparent attraction of a direct measure of soil state on Figure 33, there has been a neglect of the effect of local variation in gradation on the CSL – a single "representative" CSL has been adopted. This means that some of the 'more contractive' (loose) void ratios may be a reflection of changes in soil gradation, rather than loose soil state. This method of logging water content is a useful adjunct to CPT testing where logging of water contents is possible, but it is not a replacement for CPT soundings.

It is also common to extrude and test undisturbed silt samples in triaxial compression or cyclic simple shear. However, even if the laboratory equipment is mobilized to site to minimize the disturbance from transportation on the samples, what is universally found is that sample extrusion, trimming, and consolidation to the insitu stress level causes sample densification – what is tested is not what exists insitu. This is illustrated on Figure 33, with the laboratory tests being on samples that were substantially dilatant despite the silt insitu being contractive. The laboratory data needs to be corrected back to the insitu void ratio.

Correcting laboratory data to correspond to the insitu void ratio is not difficult. Recall that critical state models have properties that are independent of void ratio. The process is to fit a constitutive model to the laboratory test data and then to re-run the simulation at the insitu void ratio – the model then shows the effect of sample disturbance. Figure 34 provides an example of the procedure; as can be seen the modelled insitu strength, allowing for the insitu void ratio, is less than a third that measured in the laboratory test at its denser void ratio. And, what is really interesting from a liquefaction perspective is that, despite the insitu soil being far weaker than measured in the laboratory, the insitu soil still only shows modest strength loss post-peak. This method of correcting for sample densification can be applied to cyclic simple shear tests as easily as triaxial tests.

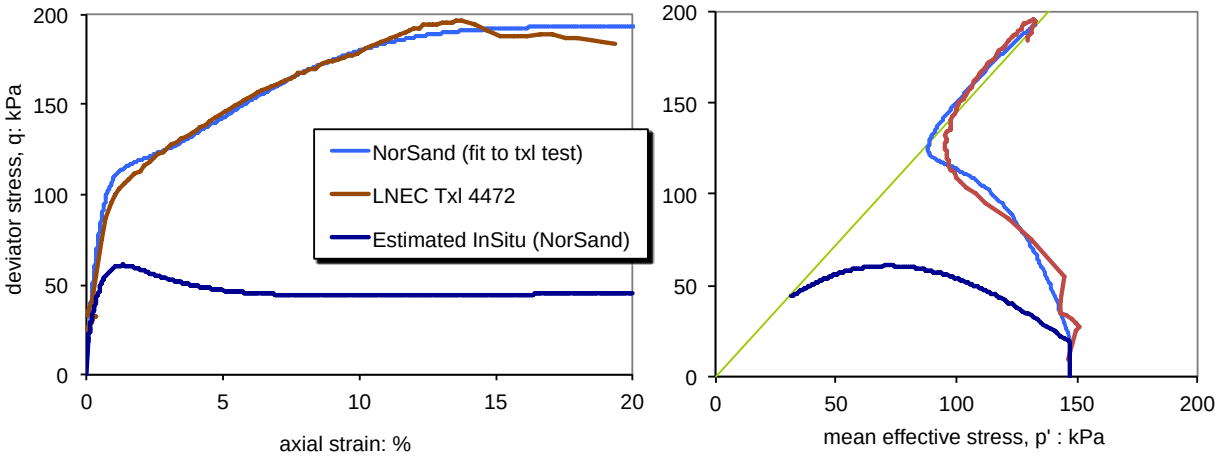

Figure 34. Correcting laboratory strengths for sample densification

ASSESSING LIQUEFACTION POTENTIAL

Given the linkage of ψ to soil dilatancy, and to detailed soil behaviour in general through Norsand or similar model, it would be reasonable to think that a site-specific calibration of Figure 32 would be a good basis for liquefaction assessment. This is true in part, but further consideration is needed.

Loose soils are always contractive in undrained shear while dense ones are always dilatant. A more complex behaviour is found with soils which are just slightly dense of the CSL, say in the range $-0.07 < \psi < +0.0$. Such soils are sometimes referred to as "compact" as a mid-way point between "loose" and "dense". An example of the behaviour of such soils in undrained simple shear is shown on Figure 35.

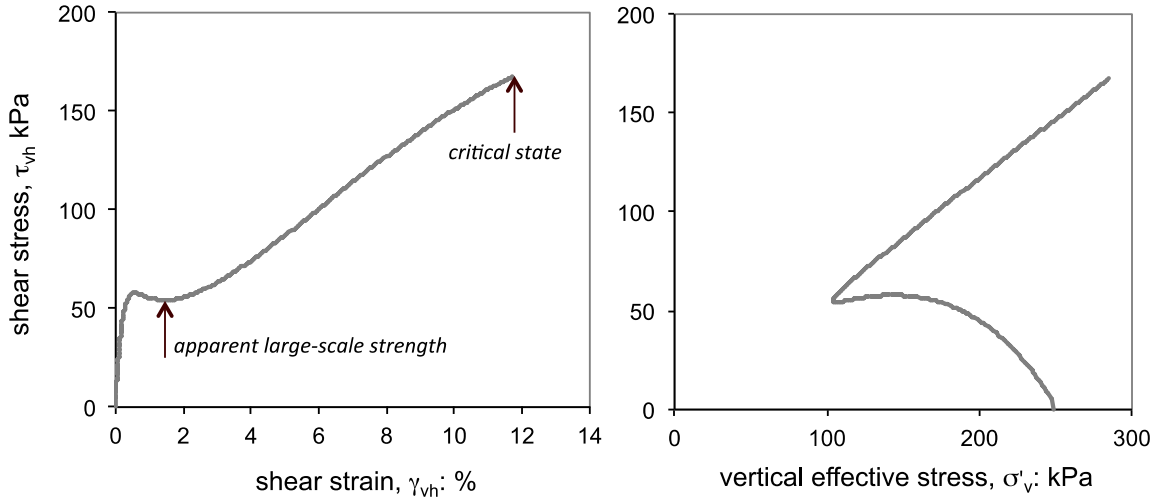

Figure 35. Example of compact silty sand behaviour in undrained simple shear

The "S" shaped stress path shown on Figure 35 is common for compact soils, and many examples of such stress paths will be found in the literature. The important consequence for practical engineering is the transient strength reduction that develops in the stress-strain behaviour; some workers refer to this lower transient strength as the *quasi-steady state*. This quasi-steady state is very different to, and can be much weaker than, the critical state strength – for example, on Figure 35 the quasi-steady state strength

is about 51 kPa versus the true undrained critical state strength at about 160 kPa. The soil goes from the reduced strength of the quasi-steady state to the true critical state as dilation develops and with substantial negative excess pore pressure.

In a laboratory test, the sample is in a uniform stress state and the undrained condition is enforced by the boundary conditions. There is no difficulty with the negative excess pore pressure being sustained, and results like that of Figure 35 are measured. In the field the situation is quite different. In the field 'undrained' is a reflection of the loading rate versus the drainage time, and that drainage time depends on the path length. In a situation where the shear stress concentrates, such as the failure zone of a limit equilibrium slip in a slope, that path length can credibly be of the order of a few metres – pore water can move in a few minutes and prevent the negative excess pore pressures developing. The expected undrained critical state strength will not be attained, with the soil failing at a looser void ratio than expected because of the pore water migration from nearby still-contracting soil. The whole process is a complex, coupled situation but it can be simply handled if the quasi-steady state is treated as the *apparent large-scale strength* as indicated on Figure 35.

This reasoning is based on constitutive behaviour. However, the conclusion has been widely known for decades. In the 1980's the idea of critical state strength that was used for the design of Franklin Falls dam in 1935 was rediscovered. In part this rediscovery was based on improved laboratory strength measurement developed by Castro (1969), although there was also a sudden realization that liquefaction was a serious geohazard following the near-catastrophic failure of Lower San Fernando Dam. Simple use of the critical state shear strength for the soil's current void ratio as "an assured minimum" was an attractive approach and resulted in what became known as the *Steady State Method*. However, calibration of this method to a few case histories quickly showed that it was substantially optimistic. The reason why the steady state school gives too optimistic strengths is just the situation shown on Figure 35 – undrained conditions cannot be enforced in real slopes and the local minimum strength controls.

Shuttle & Cunning (2008) took their NorSand based cavity expansion analysis to consider this local minimum effect, and calibrated the results for two sands (Erksak and Ticino) and one silt (Rose Creek) to produce a decision criterion for CPT data that could be used to assess whether insitu soil was vulnerable to strength loss, Figure 36. Other workers have looked at the same issue from the standpoint of case-history data (e.g. Robertson, 2010; Idriss, 2011) and there is now reasonable consensus that the decision criterion proposed by Shuttle & Cunning (2008) is broadly consistent with experience – colloquially, their decision criterion is known as "the green line". This green-line decision criterion shown on Figure 36 leads to two classes of soil liquefaction behaviour.

Soil states lying below the green-line criterion are vulnerable to strength loss; this might be triggered by an earthquake, but also by rising ground water (the trigger for the catastrophic Aberfan flowslide) or by undercutting of the slope toe (some of the Dutch dyke flowslides). Whether slides or the like develop depends on whether the post-liquefaction strength is adequate for the site geometry (you will not get a flowslide in a flat site). Practical engineering uses the post-liquefaction strengths in a limit equilibrium analysis to assess whether or not ground improvement is needed.

The 'Observational Method' must not be used for sites where soil states lie below the green-line as there will be little to no warning of impeding failure. The Aberfan slope was inspected a day before its failure, with no apparent signs of distress (e.g. tension cracks). This lack of warning can be shown computationally using NorSand.

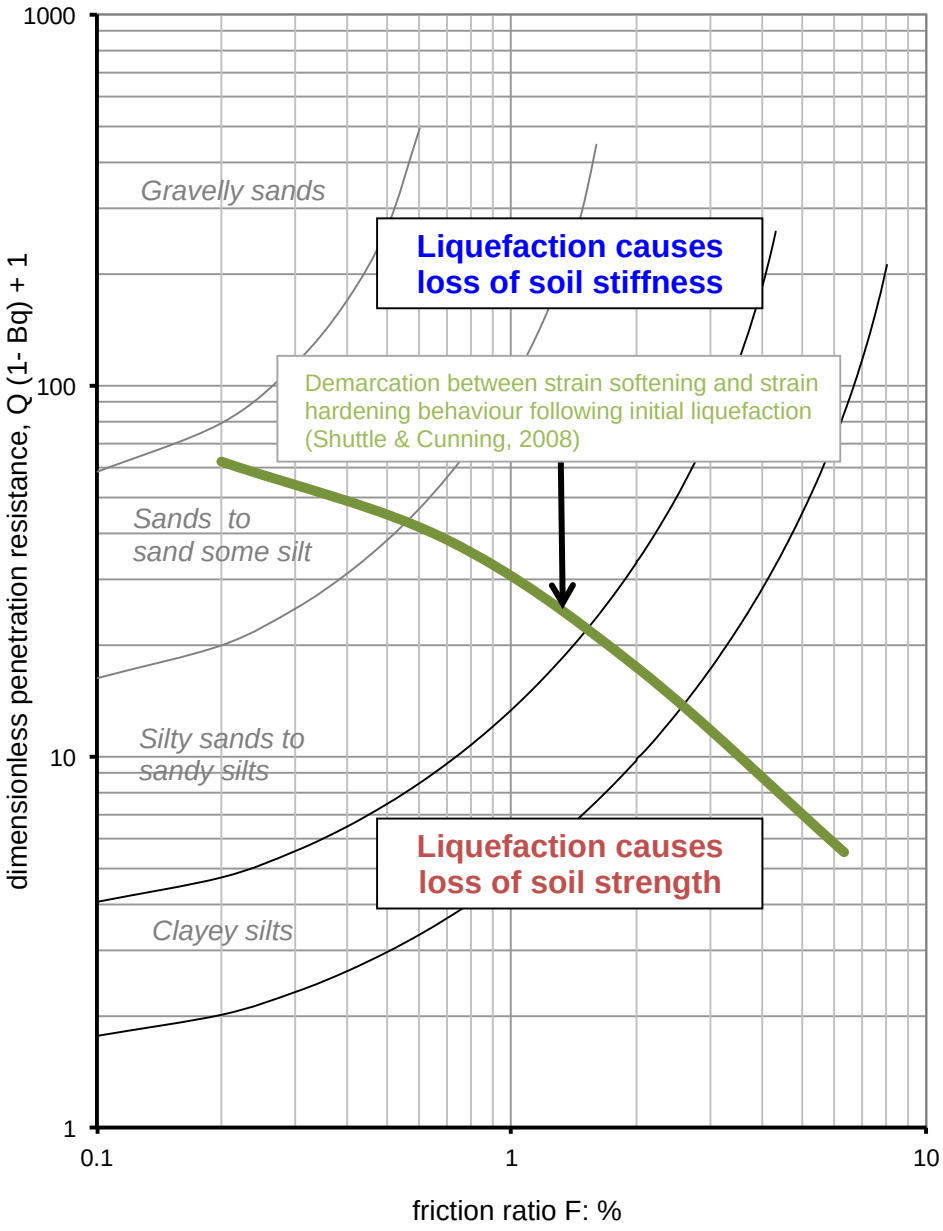

Figure 36. Liquefaction vulnerability chart (adapted after Shuttle & Cunning, 2008)

Soil states lying above the green-line criterion are limited to loss of stiffness, not loss of strength. It does not develop statically, but requires cyclic loading. Most cyclic loading is caused by earthquakes, but machine vibrations and wave action on offshore structures can result in similar effects. In the case of earthquakes, the criterion for onset of stiffness-loss is referred to as a "liquefaction triggering" criterion because cyclically induced excess pore pressure is the mechanism.

Criteria for liquefaction triggering are usually based on the case history record, where instances of liquefaction and no liquefaction in various earthquakes are assembled into a graph showing the data with a "safe" design line being developed. Laboratory tests are rarely used. How soil responds in an earthquake depends on the duration of shaking, which is largely related to earthquake magnitude(M); current practice is to bring everything to a M7.5 reference through standardized correction factors. The cyclic loading is expressed in terms of the equivalent uniform cyclic shear stress τ_{cyc} (with corrections

relating the random shaking in an earthquake to an equivalent uniform cyclic stress). This cyclic shear stress is then normalized by the vertical effective stress insitu before the earthquake, σ'_{v0}.

In the case of the back-analysis of the various case histories, the *cyclic stress ratio* (CSR) $\tau_{cyc} / \sigma'_{v0}$ experienced by a soil layer is used in plotting the experience. The same stress ratio applied to the "safe" design line is referred to as the *cyclic resistance ratio* (CRR). In either case, the CSR or CRR is related to a measure of soil state, commonly a stress level penetration resistance that has been adjusted for soil type. Although this general approach to liquefaction triggering is widely accepted, there is a vast, empirically-based, literature but no consensus regarding design trends and the subject continues to evolve.

Part of the difficulty in developing general triggering criterions is that the empirical data base only uses penetration test data as the index of soil state and only fines content as the measure of soil properties. Basic mechanical properties such as λ_{10} and G_{max} are not measured by the investigators of the various case-histories in the database, despite every constitutive model of liquefaction showing the importance of these soil properties. It would be reasonable to view the current lack of consensus as a foreseeable consequence of neglecting soil properties – there are more variables involved than used in the current regression analyses on the database. Figure 37 shows the triggering criterion for sand-like soils ($\lambda_{10} < 0.08$) based on the state parameter.

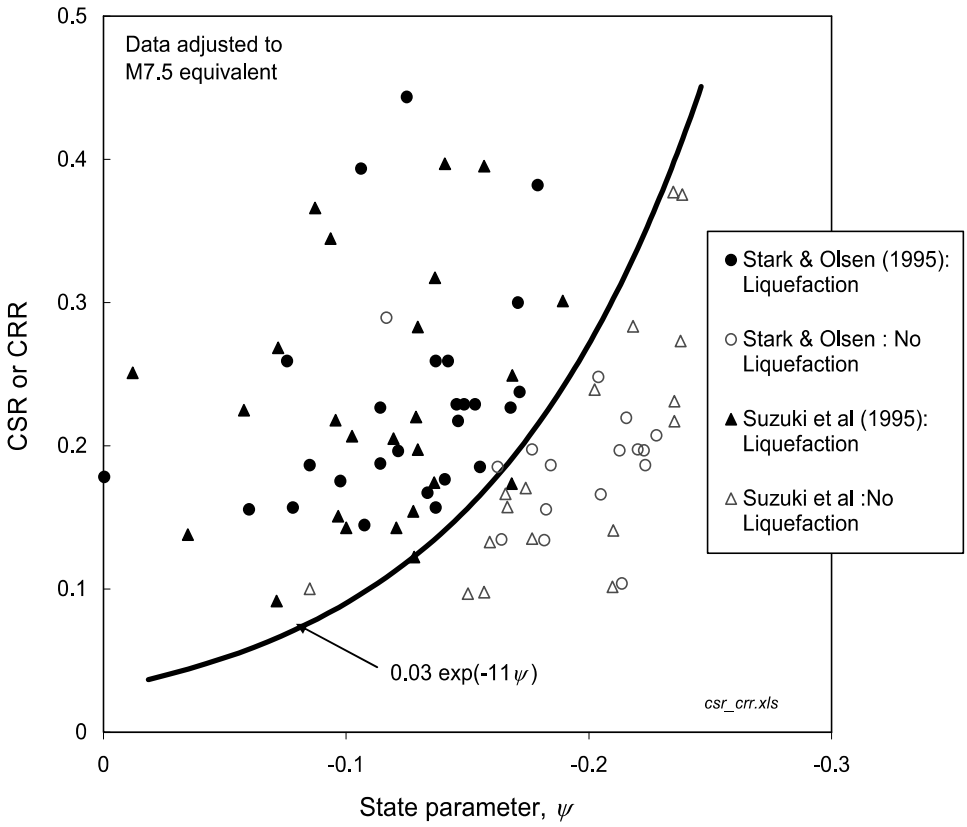

Figure 37. Onset of excess pore pressure causing stiffness-loss for sands

Constitutive models do exist for representing the nature and process of stiffness-loss during cyclic loading, indeed NorSand is one of them. However, this type of advanced modelling is rare for engineering practice. Engineering practice is usually based on avoiding the onset of softening if large strains cannot be tolerated, rather than computing the way stiffness-loss leads to accumulating displacements. Looking

at how the basis of liquefaction has changes in the past ten years it will not be long before such "advanced" modelling becomes "routine", but it would be wrong to suggest that is the case now.

CONCLUDING REMARKS

Liquefaction and theoretical soil mechanics may appear quite different aspects of geotechnical engineering, but they have been interrelated for some 80 years: the concept of the critical state came from designing a liquefaction resistant dam. However, the role of the critical state was abandoned in the 1980's, for both liquefaction studies as well as the wider constitutive modelling of soil, because of inappropriate idealizations. The situation was rectified in the 1990's with adoption of the state parameter that simply linked the critical state to soil strength and dilatancy. In turn, the modern state-parameter based models have clarified the nature of liquefaction.

A feature of the modern state-based models is that they are inevitably numerical, which acts as a deterrent to their use by practical engineers. To help address this difficulty a downloadable Excel file accompanies this lecture. The file has an open-source code implementation of *NorSand* for drained and undrained triaxial tests, together with a data set that can be used to verify how well the model works. Please do download the xls file and try it out – there is no substitute to see how predicted soil behaviour changes with changing properties and soil state. There is a "read me" file accompanying the xls file with the instructions on how to use the program.

Practically, one of the main attractions of a state-parameter basis for liquefaction is the clarity the method brings to assessment of CPT data. The effect of soil properties on the q_t-p'-e mapping can now be computed, regardless of the fines content of the soil. Essentially, any engineer can now have a site-specific calibration of the CPT for little more cost than carrying out a few triaxial tests.

Although the CPT is needed for liquefaction assessments, the CPT is only part of the story. As a minimum, about 1 in 5 CPT soundings should be done using a seismic CPT so that G_{max} is profiled at the site – a requirement that is easy enough to do and does not cost much. Soil properties will also need to be developed, whether by judgment using aspects like mineralogy and grain shape to estimate properties from testing of comparable soils or by a modest program of laboratory testing on reconstituted samples. But, however this is done, a mechanics approach does require consideration of M, N and λ_{10}.

Finally, this Šuklje Lecture has been an introduction to the wider subject of constitutive behaviour of soils and the consequences of that for engineering practice. These issues have been presented with detailed derivations in a book (Jefferies & Been, 2006; second edition pending) and a considerable amount data and programs are available as public-domain downloads (see www.golder.com/liq).

REFERENCES

Been, K. and Jefferies, M.G. (1985); A state parameter for sands. Géotechnique 35, 99-112.

Been, K. and Jefferies, M.G. (1986); A state parameter for sands: Reply to Discussion. Géotechnique 36, 123-132.

Been, K., Crooks, J.H.A. and Jefferies, M.G. (1988); Interpretation of material state from the CPT in sands and clays. Proc, Conference on Penetration Testing in the U.K., Birmingham, Thomas Telford, London, 89-92.

Been, K., Jefferies, M.G. and Hachey, J.E. (1991); The critical state of sands. Géotechnique, 41, 365-381.

Been, K., Jefferies, M.G. and Hachey, J.E. (1992); The critical state of sands: Reply to Discussion. Géotechnique, 42, 655-663.

Been K., Crooks J.H.A., Becker D.E. and Jefferies M.G. (1986); The cone penetration test in sands: Part I, state parameter interpretation. Géotechnique 36, 239-249.

Been K., Jefferies M.G., Crooks J.H.A. and Rothenberg L. (1987); The cone penetration test in sands: Part II, general inference of state. Géotechnique 37, 285-299.

Been, K., Lingnau, B.E., Crooks, J.H.A. and Leach, B. (1989); Cone penetration test calibration for Erksak (Beaufort Sea); sand: Reply to discussion. Canadian Geotechnical Journal 26, 177-182

Bishop, A.W. (1950); Discussion, Proc. Conf. Measurement of Shear Strength of Soils. Géotechnique 2, 113-116.

Carter, J.P., Booker J.R., and Yeung S.K. (1986); Cavity expansion in cohesive frictional soils. Géotechnique 36, 349-358.

Casagrande, A. (1936); Characteristics of cohesionless soils affecting the stability of earth fills. Journal of Boston Society of Civil Engineers 23, 257-276.

Chu, J. and Leong, W.K. (2002); Effect of fines on instability behaviour of loose sand. Géotechnique 52, 751-755.

Drucker, D.C., Gibson, R.E. and Henkel, D.J. (1957); Soil mechanics and work hardening theories of plasticity. Transactions American Society of Civil Engineers 122, 338-346.

Hazen, A. (1918); A study of the slip in the Calaveras Dam. Engineering News Record 81, 26, 1158-1164.

Hazen, A. (1920); Hydraulic fill dams. Transactions of the American Society of Civil Engineers 83, 1713-1745.

Hazen A. and Metcalf, L. (1918); Middle section of upstream side of Calaveras Dam slips into reservoir. Engineering News Record 80, 679-681.

Ishihara, K. (1993); Liquefaction and flow failure during earthquakes. Géotechnique 43, 351-415.

Ishihara, K., Tatsuoka, F., and Yasuda, S. (1975); Undrained deformation and liquefaction of sand under cyclic stresses. Soils and Foundations 15, 29-44.

Jefferies, M.G. (1993); NorSand: a simple critical state model for sand. Géotechnique 43, 91-103.

Jefferies, M.G., and Been, K. (2000); Implications for critical state theory from isotropic compression of sand. Géotechnique 50, 419-429.

Jefferies, M.G., and Shuttle, D.A. (2002); Dilatancy in general Cambridge-type models. Géotechnique 52, 625-637.

Jefferies, M. and Been, K. (2006); Soil liquefaction – a critical state approach.

Koppejan, A.W., van Wamelen, B.M. and Weinberg, L.J.H. (1948); Coastal flow slides in the Dutch province of Zeeland. Proc. 2nd ICSMFE, Rotterdam, Vol. V, 89-96.

Lade, P.V. and Pradel, D. (1990); Instability and plastic flow of soils. I: Experimental Observations. Journal of Engineering Mechanics 116, 2532-2550.

Li, X-S., Dafalias, Y.F., and Wang, Z-L. (1999); State dependent dilatancy in critical state constitutive modelling of sand. Canadian Geotechnical Journal 36, 599-611.

Manzari, M.T., and Dafalias, Y.F. (1997); A critical state two-surface plasticity model for sands. Géotechnique 47, 255-272.

Mroz. Z. and Norris, V.A. (1982); Elastoplastic and viscoplastic constitutive models for soils with application to cyclic loading. In Soil mechanics – transient and cyclic loads (eds. G.N. Pande and O.C. Zienkiewicz), 343-373. Wiley.

Reid, D. (2014); Estimating compressibility from the Cone Penetration Test - an update. Canadian Geotechnical Journal, In Press.

Resende, L., and Martin, J.B. (1985); Formulation of Drucker-Prager Cap Model. Journal of Engineering Mechanics 111, 855-881.

Reynolds, O. (1885); On the dilatancy of media composed of rigid particles in contact, with experimental illustrations. Philosophical Magazine 20, 469-481.

Robertson, P. (2010); Evaluation of flow liquefaction and liquefied strength using cone penetration test. J.Geotechnical & Geoenvironmental Eng. 136, 842-853.

Roscoe, K.H., and Burland, J.B. (1968); On the generalized stress-strain behaviour of 'wet' clay. In Engineering Plasticity (eds. J. Heyman and F.A. Leckie), 535-609. Cambridge University Press.

Roscoe, K., Schofield, A.N., and Wroth, C.P (1958); On the yielding of soils. Géotechnique 8, 22-53.

Roscoe, K.H, Schofield, A.N., and Thurairajah, A. (1963); Yielding of clays in states wetter than critical. Géotechnique 13, 211-240.

Rowe, P.W. (1962); The stress dilatancy relation for static equilibrium of an assembly of particles in contact. Proc. Royal Society of London, A 269, 500-527.

Schofield, A. and Wroth, C.P. (1968); Critical State Soil Mechanics. London, McGraw-Hill.

Shuttle, D.A., and Jefferies, M.G. (1998); Dimensionless and unbiased CPT interpretation in sand. International Journal of Numerical and Analytical Methods in Geomechanics, 22, 351-391.

Shuttle, D.A., and Cunning, J. (2007); Liquefaction Potential of Silts from CPTu. Canadian Geotechnical Journal 44, 1-19.

Shuttle, D.A., and Cunning, J. (2008); Reply to Discussion: Liquefaction Potential of Silts from CPTu. Canadian Geotechnical Journal 45, 142-145.

Stewart, H.R., Jefferies, M.G. and Goldby, H.M. (1983); Berm construction for the Gulf Canada Mobile Arctic Caisson. Proc. 15th Offshore Technology Conference, Paper OTC 4552.

Taylor, D.W. (1948); Fundamentals of soil mechanics. John Wiley, New York.

Tresca, H.E. (1864); Sur l'écoulement des corps solides soumis á de fortes pressions. Comptes Rendus de l'Académie des Sciences (Paris), 59, 754.

APPENDIX A – NorSand

Internal Model Variables	$\psi_i = \psi + \lambda \ln(\bar{\sigma}_{m,i} / \bar{\sigma}_m)$ *where* $\psi = e - e_c$ $\chi_i = \chi_{tc} / (1 - \chi_{tc} \lambda / M_{tc})$ $M_i = M(1 - \chi_i N \lvert\psi_i\rvert / M_{tc})$
Critical State	$e_c = \Gamma - \lambda \ln(\bar{\sigma}_m)$ *AND* $\eta_c = M$ *where…* $M = M_{tc} - \frac{M_{tc}^2}{3 + M_{tc}} \cos(3\theta/2 + \pi/4)$
Yield Surface & Internal Cap	$\frac{\eta}{M_i} = 1 - \ln\left(\frac{\bar{\sigma}_m}{\bar{\sigma}_{m,i}}\right)$ *with* $\left(\frac{\bar{\sigma}_{m,i}}{\bar{\sigma}_m}\right)_{\max} = \exp\left(-\chi_{tc}\psi_i / M_{i,tc}\right)$
Hardening Rule	On outer yield surface: $\frac{\dot{\bar{\sigma}}_{m,i}}{\bar{\sigma}_{m,i}} = H \frac{M_i}{M_{i,tc}} \left(\frac{\bar{\sigma}_m}{\bar{\sigma}_{m,i}}\right)^2 \left[\left(\frac{\bar{\sigma}_{m,i}}{\bar{\sigma}_m}\right)_{\max} - \frac{\bar{\sigma}_{m,i}}{\bar{\sigma}_m} \right] \dot{\varepsilon}_q^p$ On internal cap: $\frac{\dot{\bar{\sigma}}_{m,i}}{\bar{\sigma}_{m,i}} = -\frac{H}{2} \frac{M_i}{M_{i,tc}} \left\lvert \dot{\varepsilon}_q^p \right\rvert$ During principal stress rotation*:* $\frac{\dot{\bar{\sigma}}_{m,i}}{\bar{\sigma}_{m,i}} = -H_r \frac{\dot{\alpha}}{\pi}$

Stress Dilatancy & Plastic Strain Rate Ratios	$D^p = M_i - \eta \Rightarrow D^p_{tc} = D^p M_{i,tc} / M_i$ and $D^p_{te} = D^p M_{i,te} / M_i$ *define* $z_{3,tc} = \dfrac{2D^p_{tc} - 3}{6 + 2D^p_{tc}}$ and $z_{3,te} = \dfrac{2D^p_{te} - 6}{3 + 2D^p_{te}}$ $\Rightarrow \dfrac{\dot{\varepsilon}_3}{\dot{\varepsilon}_1} = z_{3,tc} - \left(z_{3,tc} - z_{3,te}\right) \cos(\dfrac{3\theta + 90}{2})$ *define* $a = (\sin\theta + \sqrt{3}\cos\theta)/3$, $b = -2\sin\theta/3$, $c = (\sin\theta - \sqrt{3}\cos\theta)/3$ $\Rightarrow \dfrac{\dot{\varepsilon}_2}{\dot{\varepsilon}_1} = (aD^p - 1 + \dfrac{\dot{\varepsilon}_3}{\dot{\varepsilon}_1}(cD^p - 1))/(1 - bD^p)$
Elasticity	$I_r = \dfrac{G}{\bar{\sigma}_m}$ with $K = \dfrac{2(1+\nu)}{3(1-2\nu)} G$